Evaluation of the Economic Feasibility of Core-Shell Baroplastic Polymers and a Comparison to Traditional Thermoplastic Elastomers

by

Sarah H. Ibrahim

B.S. Chemical Engineering
Massachusetts Institute of Technology, 2003

SUBMITTED TO THE DEPARTMENT OF MATERIALS SCIENCE AND ENGINEERING IN PARTIAL FULFILLMENT OF THE REQUIREMENTS FOR THE DEGREE OF

MASTER OF ENGINEERING IN MATERIALS SCIENCE AND ENGINEERING
AT THE
MASSACHUSETTS INSTITUTE OF TECHNOLOGY

SEPTEMBER 2005

Signature of Author: _____
Sarah Ibrahim
August 10th, 2005

Certified by: _____
Anne Mayes
Toyota Professor of Materials Science and Engineering
Thesis Supervisor

Accepted by: _____
Gerbrand Ceder
R.P. Simmons Professor of Materials Science and Engineering
Chair, Departmental Committee on Graduate Students

Evaluation of the Economic Feasibility of Core-Shell Baroplastic Polymers and a Comparison to Traditional Thermoplastic Elastomers

by

Sarah H. Ibrahim

Submitted to the Department of Materials Science and Engineering
on August 10th, 2005 in Partial Fulfillment of the Requirements for
the Degree of Master of Engineering in Materials Science and
Engineering

ABSTRACT

Baroplastic materials are pressure miscible systems that can be molded by the application of pressure at low/room temperature. They have the potential to replace traditional thermoplastic elastomers in many applications. To quantitatively determine the competitiveness of baroplastic materials in current markets, a detailed cost model was developed. Embedded in the cost model is a polymer flow model that predicts processing times as a function of processing pressure. The raw material cost of baroplastics was roughly estimated to input into the cost model. The results of the cost model show that baroplastics have a significant economic advantage over thermoplastic elastomers due, mostly, to the greatly reduced cycle times associated with processing baroplastic materials. Recommendations for future work include developing a more refined estimate of the raw material price of baroplastics as well as investigating the costs of more specific applications.

Thesis Supervisor: Anne Mayes
Title: Toyota Professor of Materials Science and Engineering

Acknowledgments

I would like to acknowledge and thank the many people who helped me bring this thesis to fruition. First and foremost, I extend my gratitude to my advisor, **Prof. Anne Mayes**, who truly guided me through this process. Thank you for making this project a pleasurable learning experience. I am also deeply indebted to **Juan Gonzalez-Leon** who patiently put up with my many questions and graciously showed me the ropes. I promise I won't be asking for any more batches of polymer! Speaking of batches of polymer, I would also like to thank **Sheldon Hewlett** for his tireless work with synthesis. In fact, I must express my appreciation of the entire **Mayes group** for their warm welcome and continued support. I would like extend my gratitude to **Prof. Randolph Kirchain** and **Dr. Jeremy Gregory** at the MIT Material Systems Laboratory for their advice and assistance in developing my cost model.

This acknowledgement would not be complete if I failed to mention my rock and support through the whole process: my husband, **Belal**. My command of the English language is not sufficient enough to express my gratitude to you in words. Finally, to my dear, sweet boy, **Yousef**: you are such a joy and I am thankful that I was chosen to be your mother. There was nothing more rewarding to me than coming home after a long day to your smiling face.

This project was partially sponsored by the MRSEC Program of the National Science Foundation under award DMR-0213282.

My deep gratitude to the Department of Material Science and Engineering at MIT and the American Society for Engineering Education (through the Office of Graduate Education at MIT) for their generous financial support.

Table of Contents

List of Figures

Page

List of Tables

Page

List of Symbols

α	Relative volatility of the two components in the distillation column
α_T	Thermal conductivity
$\dot{\gamma}$	Shear rate
$\dot{\gamma}_0$	Reference shear rate
η	Viscosity
η_0	Reference viscosity
ρ	Density
τ	Shear stress
τ_0	Initial shear stress
AC_L	Annual cost of labor
AC_{EN}	Annual energy cost
AC_{MA}	Annual material cost
AE	Annual energy consumption of the plant
AEC	Annual auxiliary equipment cost
AEC_I	Total auxiliary equipment cost investment
AMI	Annual material input
$APOT$	Actual paid operating time
B	Polymer flow coefficient
BC	Annual building cost
B_o	Bottoms stream exiting distillation column
B_s	Total required building space
C_{AEI}	Auxiliary equipment installation cost
C_{BS}	Cost of renting building space
CE	Average refrigeration energy needed for cooling
C_{MC}	Cost of the machine
C_{MD}	Cost of the mold
C_{MI}	Machine installation cost
C_P	Specific heat
CPM	Number of cycles per minute
CT	Compression time
CW	Average amount of cooling water needed
DLM	Number of direct laborers per machine
D_o	Distillate stream exiting distillation column
DW	Direct wage
dz	Length of the fluid element
E	Efficiency of heating and cooling
ECT	Effective cycle time
EMS	Percent expected market share
EPC	Effective annual production capacity of the plant

List of Symbols

EPV	Effective production volume
F_1, F_2, and F_3	Shear forces acting on the element of fluid
FC	Total fabrication cost
F_i	Feed stream entering distillation column
FOC	Annual fixed overhead cost
H	Height of the cake at any point in time during compression
HCT	Total time required to heat and cool the part and mold
HE	Average heating energy consumed
H_f	Final height of the part after compression
H_o	Height of the polymer cake before it is compressed
H_{PE}	Pellet height
ΔH	Difference between height of the polymer cake and final height of the part
ΔH_{vap}	Molar heat of vaporization
L	Length of the part
$\bar{L}$	Total molar flow of liquid in the column
L_{PA}	Part length
L_{PE}	Pellet length
L_T	Liquid stream recycled back into the distillation column
MC	Annual maintenance cost
MCF	Mold complexity factor
m_{cw}	Molar cooling water rate
MIC	Maintenance percent of the investment
ML	Baseline mold life
MMC	Annual main machine cost
MMC_I	Total main machine cost investment
M_{PA}	Amount of material per part
m_s	Molar steam rate
MS	Total market share
MSR	Material scrap rate for each part
mt	Mold wall thickness
MW	Molecular weight
n	Power law index
N_C	Number of part cavities in the mold
NO	Number of hours per day when no operations are taking place
N_{IW}	Number of indirect workers
N_{PM}	Number of parallel machines running at the same time
N_T	Number of tools required
OB	Overhead burden
OTM	Available operating time per machine
P	Processing pressure
PC	Annual production capacity

List of Symbols

P_E	Price of electricity
PL	Product life
PM	Profit markup
P_{MA}	Raw material price
Po	Average power consumption associated with compression
POT	Total paid operating time
PSA_{PA}	Projected surface area of the part
PU	Number of planned unpaid hours per day
PV	Annual production volume
PW	Part weight
Q	Flowrate
Q_C	Heat removed from the condenser
Q_R	Heat requirement of the reboiler
R	Reflux ratio
R_{min}	Minimum reflux ratio
ROT	Total required machine operating time
RR	Part reject rate
$RTOM$	Run-time for one machine
SA_{PA}	Surface area of the part
S_{IW}	Office space required for indirect workers
S_{MC}	Space required per machine
t	Compression time
TCT	Total cycle time
T_E	Ejection temperature
TEC	Annual tooling equipment cost
TEC_I	Total tooling equipment cost investment
T_M	Melting temperature of the material being molded
T_{MD}	Temperature of the mold
T_P	Processing temperature
T_R	Room temperature
UD	Number of unplanned downtime hours per day
V	Velocity of the element
$\bar{V}$	Total molar flow of vapor in the column

List of Symbols

V_B	Boilup ratio
V_0	Velocity of element at $y = 0$
V_{PA}	Part volume
V_T	Vapor stream at the top of the distillation column
W	Width of the part
WD	Number of working days per year
W_{PA}	Part width
W_{PE}	Pellet width
x_B	Mole fraction of more volatile component in the bottoms stream
x_D	Mole fraction of more volatile component in the distillate stream
x_n	Mole fraction of the more volatile component in the liquid phase at stage n
y	Distance from the midway point of the element to any other point
y_n	Mole fraction of the more volatile component in the vapor phase at stage n
z	Mole fraction of more volatile component in the feed stream

1.0 Introduction

1.1 Technology Review

Thermoplastic elastomers (TPEs) were first synthesized in the 1960s. The plastics community embraced this new class of polymers that provided a better alternative to crosslinked rubbers. Some of the advantages that TPEs have over crosslinked rubbers are that they are easier and faster to process, and are recyclable [1]. Their most notable disadvantage is that they are not as heat and solvent resistant as thermoset rubbers. Nonetheless, they managed to capture large and diverse markets ranging from footwear to adhesives [2].

TPEs are currently processed using melt processing, during which the polymers are heated to form a melt, molded, and then cooled down to solidify. This process has several disadvantages including the cost and environmental impact associated with heating and cooling the polymers and equipment. There is also the potential for thermal degradation of the polymers being molded [3]. TPEs are also currently not recycled.

As an alternative to melt processing, the Mayes group has synthesized a new class of polymers that can be processed at low/room temperature by the application of pressure. These materials were coined "baroplastics" [4]. Several types of baroplastics have been developed to date: (1) core-shell polymer nanoparticles that consist of uncrosslinked polybutyl acrylate (PBA) or poly 2-ethyl hexyl acrylate (PEHA) cores and polystyrene (PS) shells synthesized by two-stage emulsion polymerization, (2) block copolymers of PS/PBA and PS/PEHA synthesized by atom-transfer radical polymerization (ATRP), and (3) biodegradable block copolymers synthesized by the sequential ring-opening polymerization of lactones and lactides. The processing is achieved

by exploiting the pressure-induced miscibility of the low T_g and high T_g components. In fact, core-shell baroplastics can not be molded using melt processing methods.

The mechanical properties of both the core-shell systems and the block copolymers are controlled by varying the ratio of the high T_g and low T_g components and the nanoparticle/nanodomain size, and a wide range of mechanical behavior has been achieved [1]. Fabricated parts with higher polystyrene contents (~60 wt%) are more rigid, while parts with lower polystyrene contents (~40 wt%) are elastic and tough. The core-shell nanoparticles are also highly recyclable. In experiments where the PS/PEHA baroplastic was reprocessed 20 times, little indication of degradation could be found [1].

Currently a Grimco hydraulic press is being used to process the baroplastics. Molds are filled with unprocessed polymer powder and placed on the bottom press plate. The press plates then close to apply pressure. The pressure is maintained for a certain amount of time and then opened to remove the molded object. Since the whole procedure is done at around room temperature, the mold can be immediately removed and the molded product obtained. This process is similar to compression molding except for the processing temperature, which has to be much higher for traditional TPEs.

1.2 Motivation

Plastics processing has come a long way in the past century. With the development of innovative and more efficient processing methods, like injection molding, we have seen a corresponding increase in throughput and product quality as well as decreased costs associated with the process. However, companies are constantly pursuing methods and materials that will benefit their bottom line, either by reducing production costs or by adding some value to the

product. Baroplastics have a clear potential to do the former and perhaps, with more study, the latter. Due to the enormous volume of plastics produced, even a small differential in fabrication costs can have a significant net cost savings effect. Another motivating factor is environmental - namely the increased recyclability of baroplastics. Compared with traditional TPEs that are currently not recycled, baroplastics show great environmental promise.

1.3 Objectives

The main goal of this project is to address the economic feasibility of market integration of baroplastics. This was done by developing a quantitative analysis of the costs associated with synthesizing the polymers and processing them, and comparing those with the costs associated with synthesizing and processing competing traditional TPEs. A cost model of compression molding was developed to capture the unique features of low temperature processing. A theoretical model that predicts processing time as a function of processing pressure was developed and validated experimentally. The mechanical properties of the molded products were tested to obtain a quantitative standard for whether they were successfully processed or not. Finally, an analysis of the energy and fixed costs associated with processing were assessed. After looking at each component of the analysis separately, and as a whole, recommendations are made on the feasibility of market integration.

2.0 Background

2.1 Plastics

Plastics are made from polymers, long chains of repeating hydrocarbon units. Plastics can be classified into two groups: thermosets and thermoplastics. Thermosets can be heated and molded into a shape, but then cannot be remolded again. An example of a thermoset plastic is epoxy resin commonly used in applications such as adhesives/coatings and building and construction. Thermoplastics, on the other hand, once formed, can be reheated and remolded over and over again. Therefore, by definition, thermoplastics can be recycled. They are also easier and faster to process. Some examples of thermoplastics include PVC, polyethylene, ABS, nylon, and polypropylene, which are commonly used for packaging and building and construction applications. Thermoplastic elastomers (TPEs) are materials that have the mechanical properties of a rubber, while maintaining the processing advantages of thermoplastics.

2.1.1 Market

The Freedonia group reports that TPEs currently hold a $1.9 billion market in the US and a $5.8 billion market globally. The expected market growth rate is 6% annually through 2007 [2]. The current largest market for TPEs is the automotive industry and the fastest growing markets are the consumer and sporting goods markets. Commonly used objects that are made out of TPEs include: gaskets, stoppers, valves, bumpers, wheels, fuel line covers, shoe soles/heels, wrist straps, airbag doors, cosmetic cases, handles, pushbuttons, and knobs [5].

2.2 Processing

2.2.1 Compression Molding

Compression molding is one of the most common processing techniques used to make parts out of thermosets. It is also used, but less commonly, to process thermoplastics. In most cases, as can be seen in Figure 2.1, a pre-heated polymer charge is placed in a heated mold, which is then closed to apply pressure to the charge and force it to take the shape of the mold. The charge is preheated to reduce the temperature difference between it and the mold. The polymer, due to the pressure and temperature, becomes fully cured and solidifies in its shaped form, and can be ejected. Because cycle times in compression molding can take up to several minutes, industrial processes will usually use multi-cavity molds to increase the production rate [6].

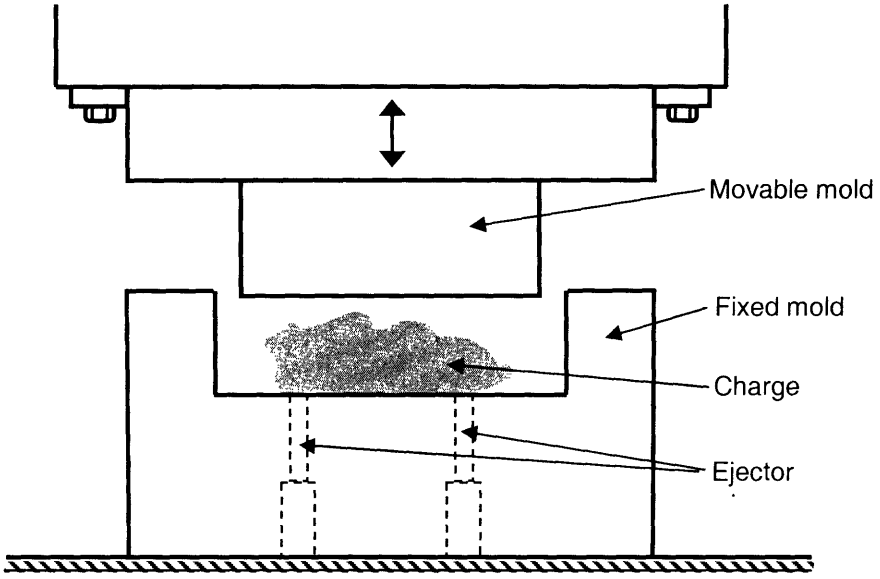

Figure 2.1 Example of industrial scale compression molding equipment

Baroplastics, however, as described earlier, do not need to be heated in order to be processed. Rather, the applied pressure, as the name implies, is enough to shape them. This can greatly affect the throughput of the process while also reducing costs.

2.3 Theory

In order to develop a useful cost model, an understanding of the underlying mechanisms involved in the process is important. By analyzing polymer flow behavior during processing, we can determine, theoretically, how long it takes for the polymer to fill the mold for a given applied processing force. The analysis will be based on the production of a simple box top.

2.3.1 Polymer Flow

For the purpose of this analysis, it will be assumed that a "cake" shaped charge is placed between the molding plates. A constant, uniform force is applied to the upper mold plate resulting in a pressure gradient, as shown in Figure 2.2.

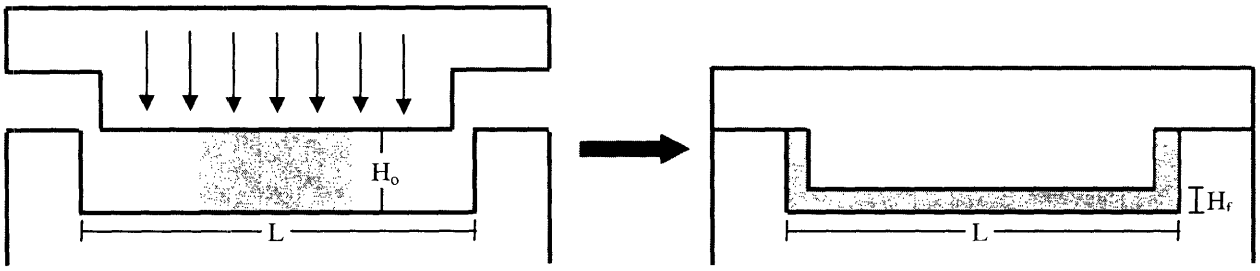

Figure 2.2 Diagram of pressed part

In the proposed model, H_o is the height of the polymer cake before it is compressed, H_f is the final height of the part after compression, and L is the length of the part.

As a simplification, it will be assumed that the part is flat and the effect of the corners is negligible. Because of symmetry, analysis can be carried out on half of the system and then

generalized to give an accurate description of what happens in the system as a whole. An element of fluid in the channel is analyzed as seen in Figure 2.3 below.

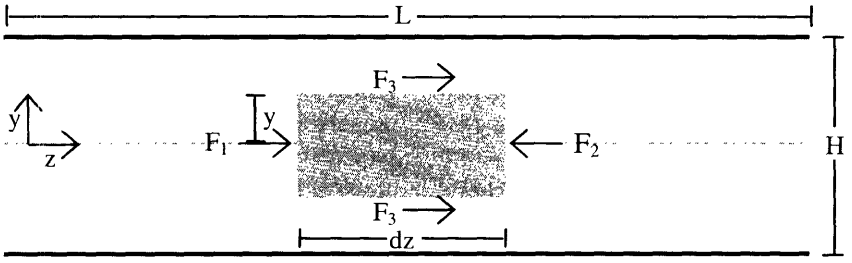

Figure 2.3 Analysis of element of fluid

F_1, F_2, and F_3 are the shear forces acting on the element of fluid, dz is the length of the fluid element, y is the distance from the midway point of the element to any other point, and H is the height of the cake at any point in time during compression.

By performing a force balance on the element and taking into account constitutive relations as well as geometrical effects (see Appendix A for a detailed derivation), we get the following expression relating the processing force to the processing time:

$$F = 2WL^{n+2}\left(\frac{\eta_0}{\dot{\gamma}_0^{n-1}}\right)B\frac{\Delta H^{-(n+1)}}{t^n} \tag{2.1}$$

where W is the width of the part, n is the power law index, $\dot{\gamma}_0$ is the reference shear rate, η_0 is the reference viscosity, n is the power law index, ΔH is the difference between the height of the polymer cake, H_o, and the final height of the part, H_f, t is the compression time, and B is a coefficient defined as:

$$B = \frac{2^{n+1}}{(n+2)}\left(\frac{2n+1}{n+1}\right)^n \tag{2.2}$$

The term $\eta_0 / \dot{\gamma}^{n-1}$ can be determined experimentally using a rheometer. The goal of performing the polymer flow analysis is to find an expression that relates processing time to the processing pressure (or force). This allows us to optimize the processing parameters for a given application as well as determine what factors most influence the results. We can also integrate the results of this analysis into the cost model to allow us to automatically determine cycle time as a function of the different parameters.

2.3.2 Materials

Core-shell baroplastics are spherical nanoparticles that contain either a polybutyl acrylate (PBA) or poly 2-ethyl hexyl acrylate (PEHA) core and a polystyrene shell. The weight fraction ratio of polystyrene to PBA or PEHA largely determines the mechanical properties of the material. In order to have a product that is not too tacky or too brittle, polystyrene weight fractions are varied between 40 and 60%. Nanoparticle sizes vary from 40 to 200 nm depending on the amount of surfactant used during synthesis.

A fabricated part composed of a 50/50 PS/PBA core-shell baroplastic will appear transparent. The material properties of a 51/49 PS/PBA core-shell system with a core diameter of 58.1 nm and a core-shell diameter of 72.2 nm were studied. A stress-strain graph for the system processed at 5000 psi and 25°C for 5 minutes can be seen in Figure 2.4. The stress-strain curves were generated by molding a rectangular part and then cutting out dog-bone shaped pieces. The dog bone shaped pieces were then placed in an Instron machine (Model 4501) which generated the curves. Based on the stress-strain data collected, the modulus was calculated to be around 95 MPa.

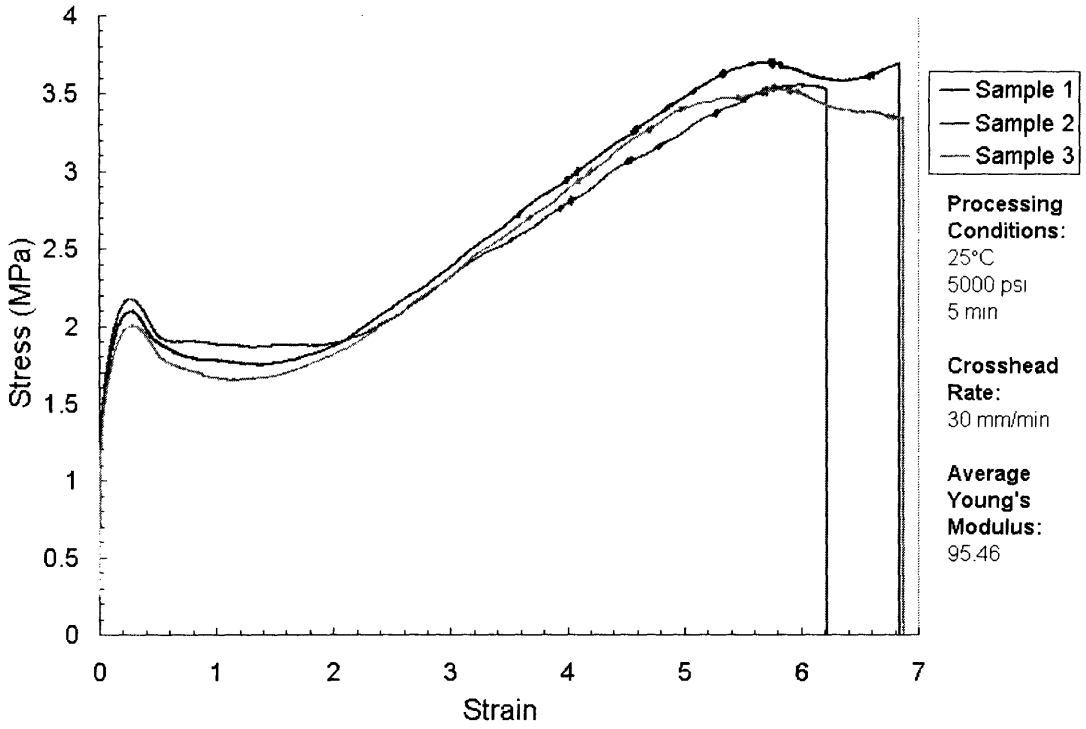

Figure 2.4 Stress-strain curves for PS/PBA core-shell baroplastics with a weight fraction ratio of 51:49 and core/core-shell diameters of 58.1/72.2 nm processed at 5000 psi and 25°C for 5 min.

It was also shown that the modulus is not a function of how long the part is processed for. This can be seen in Figure 2.5 where the average modulus of a 51/49 PS/PBA core-shell material was measured for parts processed for different times. The parts that are fully processed at very short times have comparable mechanical properties to those that have been processed longer.

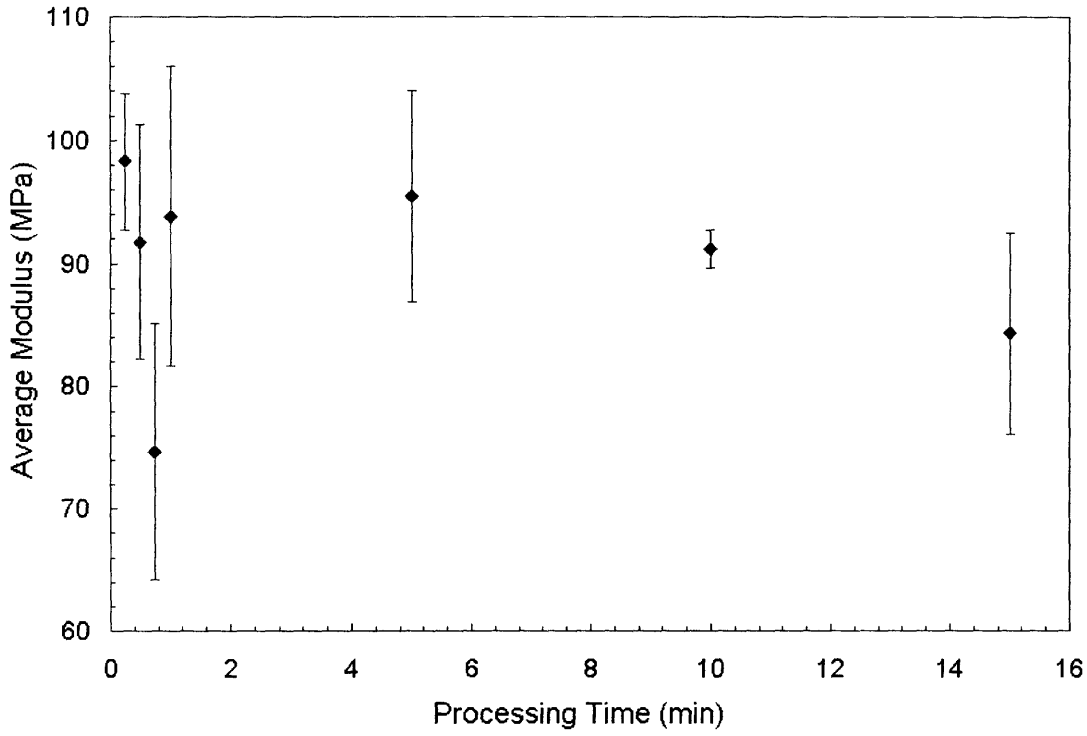

Figure 2.5 Graph of the average modulus as a function of processing time for a 51/49 PS/PBA core-shell baroplastic processed at 5000 psi and 25°C. Each data point represents the average modulus of three samples.

2.3.3 Experimental Determination of Key Material Parameters

The two material property inputs in Eqn 2.1 were experimentally determined using a rheometer (Rheometric Scientific ARES). The baroplastic polymers were compression molded in a press into sheets (at a compression pressure and temperature of 5000 psi and 30°C for 5 minutes) and 1" diameter disks were cut out. The disks were then placed in the rheometer and the apparent viscosity was measured as a function of different shear rates. The data obtained was then fit according to the power relation [6]:

$$\eta = \left(\frac{\eta_0}{\dot{\gamma}_0^{n-1}} \right) \dot{\gamma}^{n-1} \tag{2.3}$$

Figure 2.6 is a graph of the apparent viscosity as a function of the shear rate for a PS/PBA (51:49 weight fraction ratio) core-shell baroplastic at a temperature of 30°C (the lowest temperature setting on the rheometer) plotted on a log-log scale. Based on the data fit, the term $\eta_0/\dot{\gamma}^{n-1}$ was found to be equal to 1.76×10^6 Pa·sec^n and the power law index, n, was found to be 0.18.

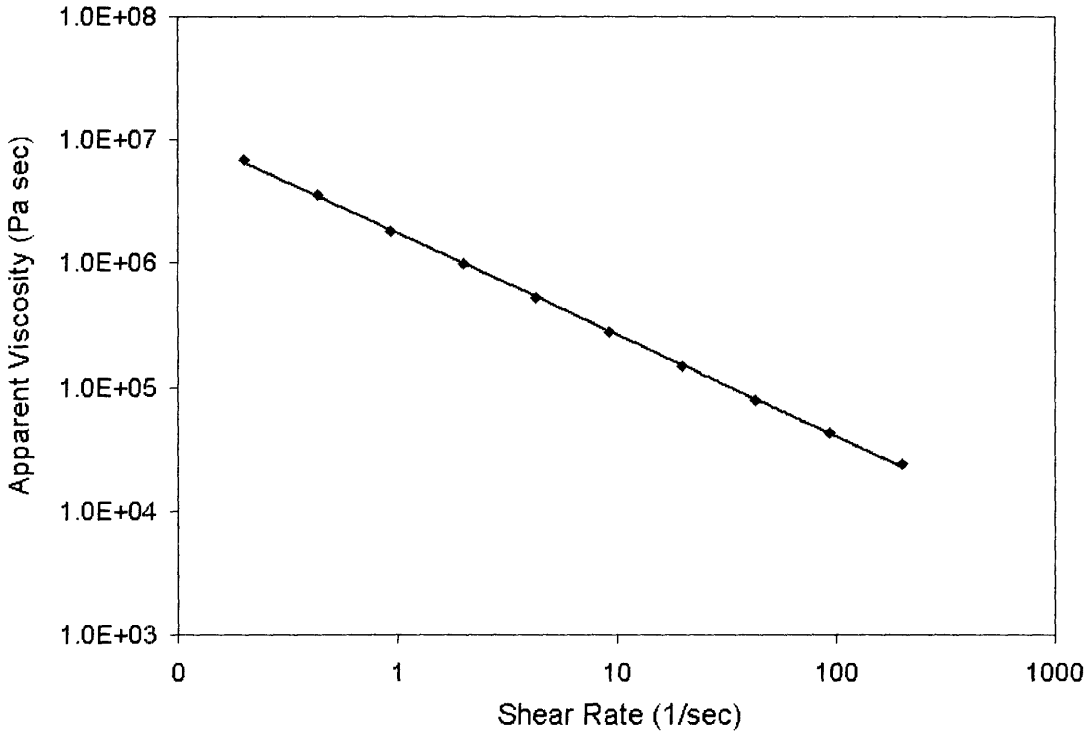

Figure 2.6 Apparent viscosity as a function of the shear rate for a PS_{50}/PBA_{50} baroplastic at 30°C. The data is fitted to the power law equation: $\eta = 1760185.77\dot{\gamma}^{-0.82}$.

Figure 2.7 depicts predicted processing pressure vs. processing time for different values of the power law index, 'n' (for $\eta_0/\dot{\gamma}^{n-1} = 1.76 \times 10^6$ Pa·sec^n) and Figure 2.8 compares processing pressures and times for varying values of the term, $\eta_0/\dot{\gamma}^{n-1}$ (for $n = 0.18$). The graphs show that the process is highly sensitive to both the power law index and the viscosity. An order

of magnitude difference in the apparent viscosity leads to a ten-fold difference in the processing pressure for a given processing time. An order of magnitude increase in the power law index leads to a substantial decrease in the processing pressure for a given time. It follows that in order for the model to be accurate, these two values must be precisely measured for a given material.

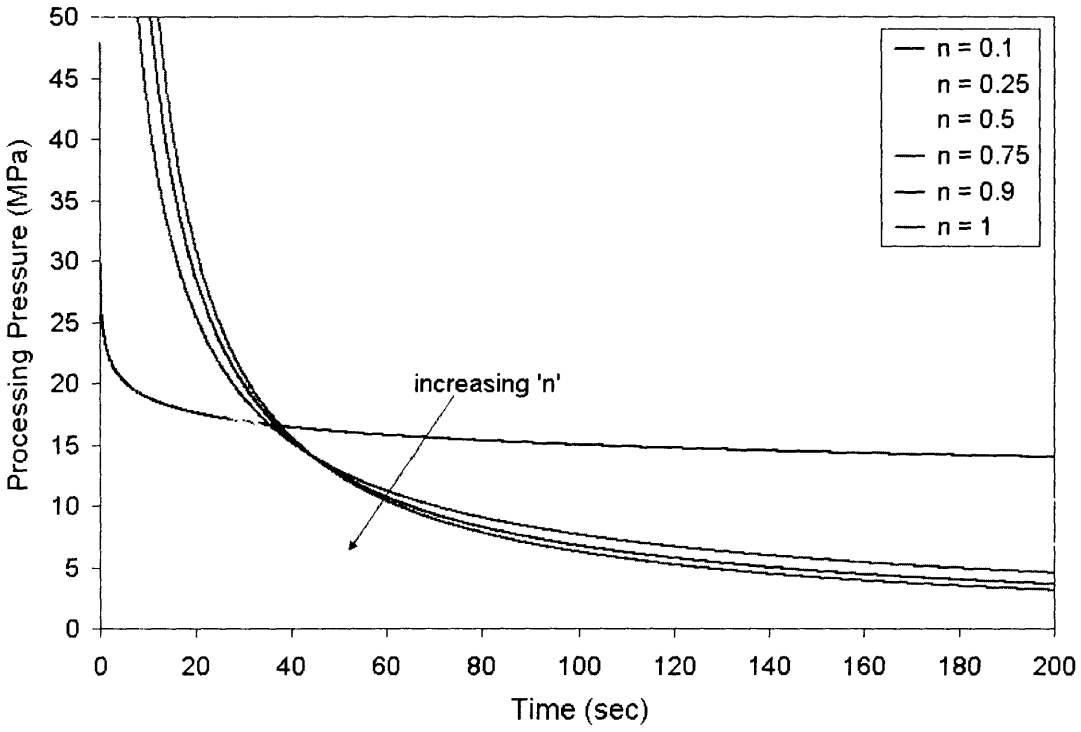

Figure 2.7 Theoretical processing pressure vs. processing time for different values of the power law index '*n*' for a 5 × 5 × 1 cm box top part.

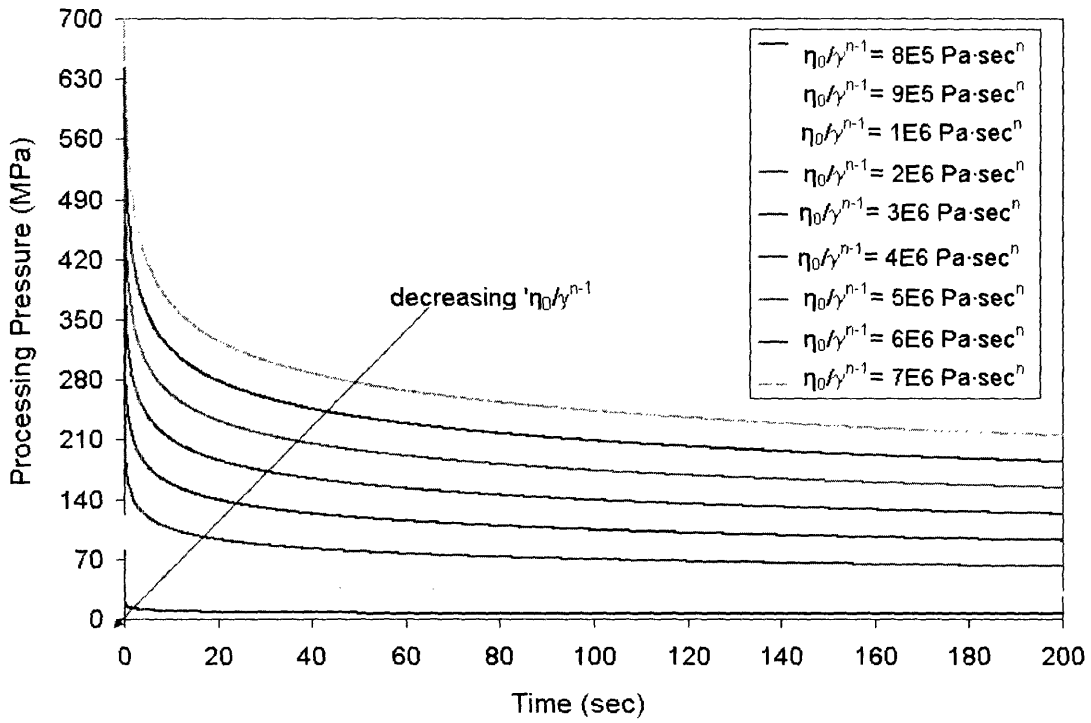

Figure 2.8 Theoretical processing pressure vs. processing time for different values of the viscosity 'η_0' for a 5 × 5 × 1 cm box top part.

2.3.4 Model Validation

The model described in Section 3.2.1 assumes that a pre-formed polymer pellet is placed in the mold and compressed. The model then predicts how long it will take for the polymer to reach both ends of the mold, thereby filling it. In order to make a reasonably accurate comparison to the model, experiments were carried out where pellets of known dimensions were placed in a rectangular mold and processed at different pressures and times. The pellets were made by processing a 65/35 PS/PEHA (with core/core-shell diameters of 61/78 nm) core-shell system into flat sheets and then cutting out rectangular pieces with dimensions of 1.9 x 3.5 x 0.56 cm. Five rectangular pieces were then stacked on top of each other to bring the pellet weight to approximately 1.7-1.9 g. Each pellet was placed in the center of the mold, processed, and the resulting length of the part recorded. The part was considered fully processed when the length of the processed part was equal to the length of the mold (6.9 cm).

The material properties of the 65/35 PS/PEHA system needed as inputs for the model could not be accurately measured using a rheometer. There was too much variability in the results for the data to be reliable. The variability was most likely a result of slippage between the plates of the rheometer and the polymer disks, which results in inaccurate viscosity readings. Instead, the material properties were measured using an extruder setup, where polymer was placed in a mold with a small circular orifice and compressed at different pressures using a piston for a given amount of time. The length of polymer extrudate was then measured for each processing pressure. The shear rate and apparent viscosity were calculated from the data collected and plotted as seen in Figure 2.9. Based on the data fit, the term $\eta_0/\dot{\gamma}^{n-1}$ was found to be equal to 5.42×10^6 Pa·sec^n and the power law index, n, was found to be 0.357.

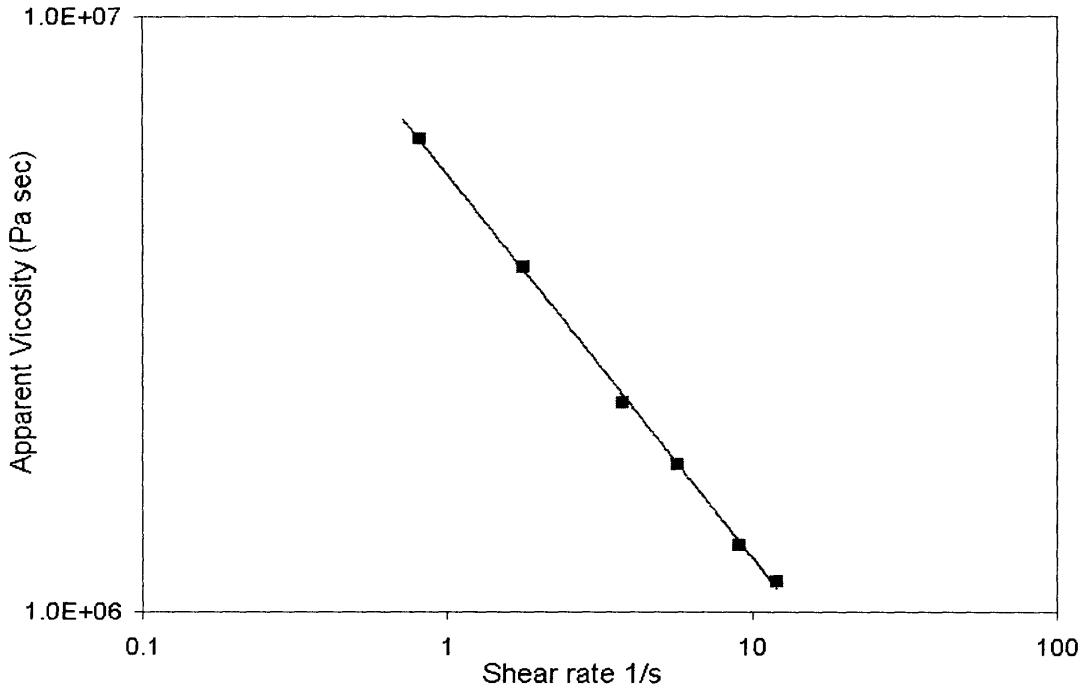

Figure 2.9 Graph of the apparent viscosity as a function of the shear rate for a $PS_{65}/PEHA_{35}$ baroplastic at 25°C. The data is fitted to the power law equation: $\eta = 5420791.11\dot{\gamma}^{-0.643}$.

Figure 2.10 shows a comparison between the theoretical model predictions and experimental values for the 65/35 PS/PEHA core-shell system. Both data sets seem to follow the same trend, but the theoretical model under-predicts the required processing pressure for a given processing time. The discrepancy can be due to several reasons. The first possible reason is that the no-slip assumption used in the model does not apply. Any friction between the polymer and the mold will increase the amount of time needed to fill the mold. Another reason is the error associated with measuring the material properties required for the model.

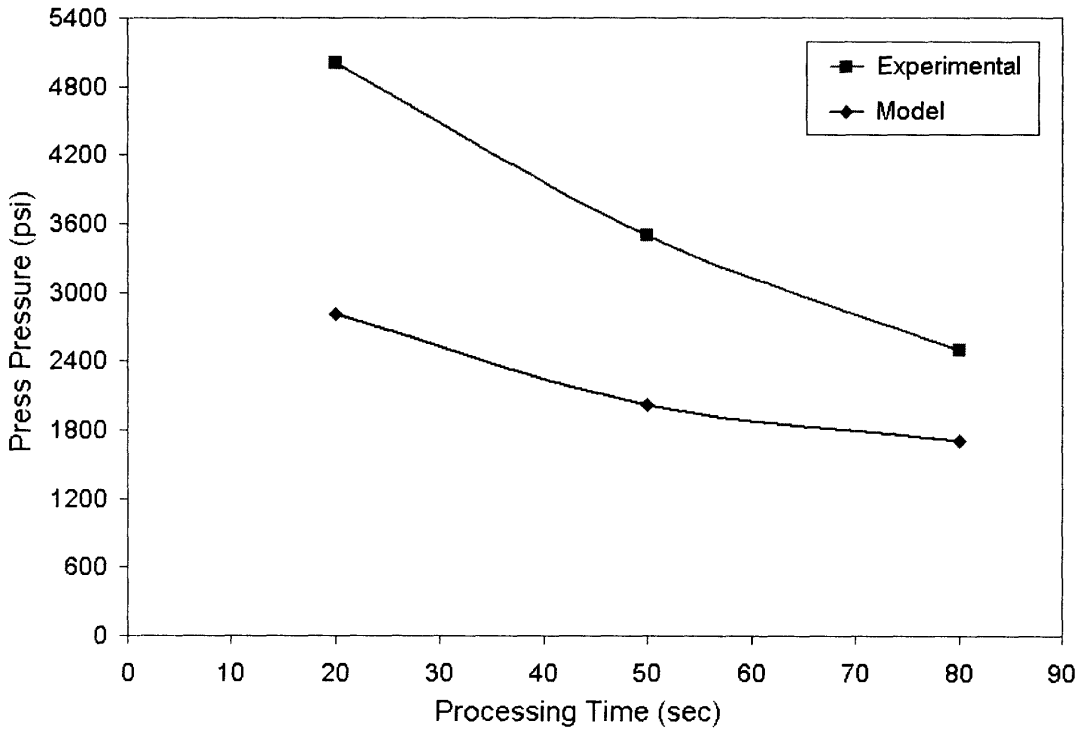

Figure 2.10 Comparison between theoretical predictions of processing pressure vs. time and experimental values.

3.0 Intellectual Property

In performing an IP search, the two main patentable aspects of the technology were considered: synthesis and structure. Methods of searching included using the US Patent and Trademark Office's (USPTO) search engine, examining the patents referenced in the Baroplastic patent, and using SciFinder to pinpoint relevant patents.

3.1 Current IP

A patent on baroplastics materials was issued to Prof. Mayes and other members of her research group in October 2003 (Patent # 6,632,883, Filed February 2001). This patent covers baroplastics that have a block copolymeric structure. The authors listed on the patent are Anne Mayes, Anne Valerie Ruzette, Thomas Russell, and Pallab Banerjee. The patent covers aspects from structure to processing, making it broad in the area of low temperature plastics processing. It also, at a very basic level, claims a thermodynamic criterion for polymer systems to be baroplastics.

Another patent on structured baroplastic materials was filed in January 2003 (Application # 60/438,445). This patent covers the core-shell nanoparticle structures. The authors listed on the patent are Anne M. Mayes, Sang Woog Ryu, Metin Acar, and Juan Gonzalez. This patent also covers aspects from structure to processing.

3.2 IP Search Results

3.2.1 Synthesis

Core-shell nanoparticles are synthesized by emulsion polymerization. The first patent on emulsion polymerization was filed in Germany in the 1930s. Much more has been learned about this synthesis process since that first patent was filed and it has gone from being a mere scientific curiosity to a widely used polymerization technique. There are many patents filed that claim variations of this method. One particular patent by Blankenship et al. at Rohm and Hass Company (Patent # 6,020,435 (2000): Process for preparing polymer core shell type emulsions and polymers formed therefrom) stands out. However, in its claims, the patent narrowly defines the materials used in the emulsion, making it not problematic in terms of baroplastics synthesis.

3.2.2 Structure

Many patents on core-shell systems were found, especially in the context of ink-jet printing and as impact modifiers for thermoplastic resins. However, all of the patents found either covered nanoparticles that were much larger than the baroplastic nanoparticles being synthesized, or specify crosslinked cores as seen in the patent by Ferry et al. at Rohm and Hass Company (Patent # 3,985,703 (1976): Process for manufacture of acrylic core/shell polymers). The patent pending for baroplastic structured materials explicitly specifies an uncrosslinked core and an uncrosslinked shell.

3.3 Proposed IP Strategy

Based on the results of the IP search, the substantial start-up manufacturing costs associated with plastics processing, and the risk associated with entering into high-volume markets, it is

proposed that the technology be licensed to established plastics processing companies. As the cost model discussed further in this paper shows, this technology has the potential to be more cost-effective than traditional thermoplastics. This will make procuring a license to produce and process baroplastics very attractive to companies that would like to establish or maintain a competitive advantage in the market.

4.0 Business Model

4.1 Cost Model

The final part of this study was to bring together the experimental and theoretical analyses into a cost model that would allow for the assessment of the economic feasibility of baroplastics and whether they provide any real economic advantage over thermoplastics currently used today.

4.1.1 Raw Material Cost

In order to approximate the raw material cost of the core-shell baroplastics, bulk price estimates were obtained for the chemicals used in the synthesis. The synthesis method currently used is a two-stage emulsion polymerization. The solvents used are methanol, acetone, and de-ionized water. The monomers are styrene and either butyl acrylate or 2-ethy hexyl acrylate. 2,2 azobis (2 methyl propionamide) dihydrochloride (VSO), is used as an initiator for the first stage of the emulsion polymerization. Either tetradecyltrimethyl ammonium bromide (TTAB) or hexadecyltrimethyl ammonium bromide (HTAB) is used as a surfactant in both stages. Finally, a chain transfer agent, 1-Dodecanethiol, is used in the second stage of the emulsion polymerization. The materials, amount required, and their bulk prices can be found in Table 4.1.

Table 4.1 Chemicals used in PS/PBA core-shell synthesis and their prices.

Chemical	Unit	Price ($/g or $/L)	Total Amount needed for 1 batch (40 g produced)	Amount needed per gram of product synthesized	Total Price ($/g of product produced)
Methanol	L	2.38E-01	1.00E+00	2.50E-02	5.94E-03
Acetone	L	1.32E-03	5.06E-03	1.26E-04	1.67E-07
HTAB	g	3.50E-02	4.50E+00	1.13E-01	3.94E-03
Butyl Acrylate	g	2.09E-03	2.00E+01	5.00E-01	1.05E-03
Styrene	g	1.54E-03	3.00E+01	7.50E-01	1.16E-03
VSO	g	1.30E-01	2.00E-01	5.00E-03	6.50E-04
1-Dodecanethiol	g	1.36E+01	1.00E-04	2.50E-06	3.39E-05
				TOTAL ($/g)	**0.013**
				TOTAL ($/kg)	**12.770**
				TOTAL ($/lb)	**5.792**

Bulk prices for methanol, acetone, and styrene were obtained from the January 10, 2005 issue of *The Chemical Market Reporter* [7]. Butyl acrylate and 2-ethyl hexyl acrylate bulk prices are from a BASF December 2004 press release. Finally, bulk prices for HTAB and VSO were obtained through a quote from Sigma-Aldrich.

Based on the numbers in Table 4.1, the cost of core-shell baroplastics would be roughly $6-7/lb if we assume that the fixed and energy costs are around 20% of the raw material cost. However, methanol, which is the largest contributor to the raw material cost, would most likely be recycled and re-used in practice. Methanol is used to extract the core-shell polymer at the end of the synthesis. The polymer, which precipitates out of solution in the presence of methanol, is then filtered out. The result is a mixture of methanol and water with trace amounts of acetone. Therefore a distillation column that separates methanol from water was designed and its cost estimated. Details of the distillation design and cost can be seen in Appendix C. Recycling the

methanol brings the core-shell baroplastic cost down to around $4/lb. This is still a very conservative estimate since the synthesis procedure has not been optimized.

4.1.2 Manufacturing Cost

For the sake of this analysis, a representative styrenic thermoplastic elastomer, with properties closest to the baroplastic materials being studied, was assumed. Since this analysis is intended to be a comparison between the processing of two different materials with a wide range of application, a relatively simple part, a small box top, for which a mold was already available, was chosen for study. The results can then be used to determine whether looking at more complex parts with market applications is advisable.

As can be seen in Table 4.2, there are several main differences in the fabrication of baroplastics and thermoplastics. The first, and most significant difference, is the cycle time. Traditional thermoplastics take much longer to process because of the added heating and cooling times. To calculate the heating and cooling times for thermoplastics, correlations developed in the MIT Materials Systems Laboratory [8] were used. This difference in cycle time has the effect of causing a significant difference in the variable costs associated with manufacturing.

The second main difference between processing baroplastics and thermoplastics is the price of the unprocessed polymer. As discussed in Section 4.1.1, so far, the conservative estimate of the raw material price of baroplastics is around $0.009/g. However, the actual bulk price will likely be much lower in practice. Styrenic thermoplastic elastomers cost around $1.50/lb ($0.0033/g).

The final main difference is the predicted mold life associated with processing baroplastics versus processing thermoplastics. The heating and cooling steps involved in

thermoplastics processing introduce additional sources of stress to the mold and cause the mold to fail faster than it would in the absence of those stresses. It is very difficult to quantify with any degree of accuracy how the mold life will be impacted by the lack of heating and cooling and no data was found in the literature. For the purposes of this analysis, a 50% increase in mold life for baroplastics processing was assumed. The specific inputs that went into the baroplastic cost model are shown in detail in Appendix D.

Table 4.2 The three major differences in processing baroplastics and traditional thermoplastics

Processing Pressure = 30 MPa	Baroplastics	Traditional TPEs
Cycle Time	15 sec.	150 sec.
Material Costs	~ $4/lb	~ $1.5/lb
Mold Life	1,500,000 parts	1,000,000 parts

Figure 4.1 shows a breakdown of the costs associated with baroplastics processing. Material costs account for the largest percentage of the total cost with labor and energy costs coming in second and third. The total cost of the part, including a 50% profit markup, is found to be $0.27 assuming an annual production volume of 1,000,000 parts.

VARIABLE COSTS	per piece	per year	percent
Material Cost	$0.017	$17,340.01	9.67%
Energy Cost	$0.013	$12,631.12	7.05%
Labor Cost	$0.098	$98,453.76	54.92%
Total Variable Cost	**$0.13**	**$128,424.90**	**71.64%**

FIXED COSTS	per piece	per year	percent	investment
Main Machine Cost	$0.011	$10,710.93	5.97%	$81,468.19
Auxiliary Equipment Cost	$0.002	$1,785.16	1.00%	$13,578.03
Tooling Cost	$0.020	$20,326.04	11.34%	$77,051.69
Fixed Overhead Cost	$0.012	$11,646.63	6.50%	
Building Cost	$0.005	$4,506.82	2.51%	
Maintenance Cost	$0.002	$1,866.45	1.04%	
Total Fixed Cost	**$0.05**	**$50,842.03**	**28.36%**	**$158,519.88**

Total Fabrication Cost	$0.18	$179,266.93	100.00%

Profit Markup	50%
Total cost of Part	$0.27 /part

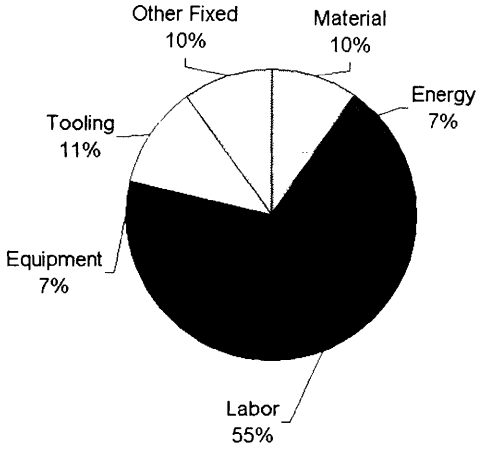

Figure 4.1 Tabulated costs of processing a baroplastic material and pie graph showing the total cost broken down into its components.

Figure 4.2 shows a breakdown of the costs associated with thermoplastic processing. Labor costs account for the largest percentage of the total cost, with equipment and energy costs coming in second and third. The total cost of the part, including a 50% profit markup, is found to be $0.44. Initially, it was thought that a difference in energy costs (from the heating and cooling steps) would be the biggest advantage of baroplastics over thermoplastics. The model calculates energy savings of around 6×10^5 BTU (175 kwh) per million parts by using baroplastic materials. However, the results of the cost model show that labor and tooling costs, are, in fact, much more important than energy costs. This is due to the substantial difference in cycle times associated with the different materials. In order to maintain the same throughput with a higher cycle time, more machines and hence more laborers must be used. The added energy costs due to heating and cooling are negligible in comparison with the added tooling and labor costs.

VARIABLE COSTS	per piece	per year	percent	
Material Cost	$0.006	$6,358.01	2.16%	
Energy Cost	$0.013	$12,998.38	4.42%	
Labor Cost	$0.151	$150,978.36	51.28%	
Total Variable Cost	**$0.17**	**$170,334.74**	**57.86%**	
FIXED COSTS	**per piece**	**per year**	**percent**	**investment**
Main Machine Cost	$0.043	$42,843.72	14.55%	$325,872.77
Auxiliary Equipment Cost	$0.007	$7,140.62	2.43%	$54,312.13
Tooling Cost	$0.034	$33,876.74	11.51%	$128,419.49
Fixed Overhead Cost	$0.028	$28,419.57	9.65%	
Building Cost	$0.007	$7,227.28	2.45%	
Maintenance Cost	$0.005	$4,554.42	1.55%	
Total Fixed Cost	**$0.12**	**$124,062.35**	**42.14%**	**$454,292.26**

Total Fabrication Cost	$0.29	$294,397.09	100.00%

Profit Markup	50%
Total cost of Part	$0.44 /part

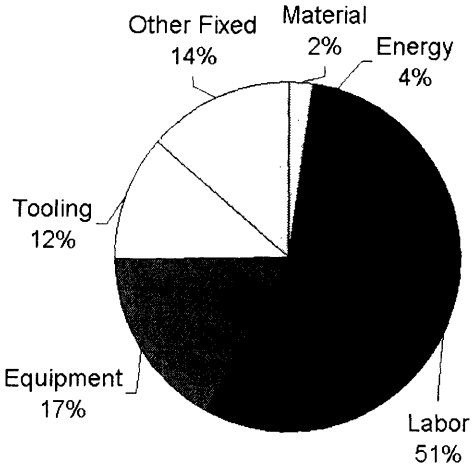

Figure 4.2 Tabulated costs of processing a thermoplastic material and pie graph showing the total cost broken down into its components.

The next step was to determine if there is a processing pressure that minimizes the cost of the part. Figure 4.3 shows the total, variable, and fixed costs per part graphed as a function of the processing pressure. There is a distinct minimum to the curve. This is because at very low processing pressures, the cycle time is very high, which leads to an increase in labor and machine costs. At very high processing pressures, the energy requirement begins to dominate. That is why the shape of the total cost per part curve primarily mimics the variable cost curve.

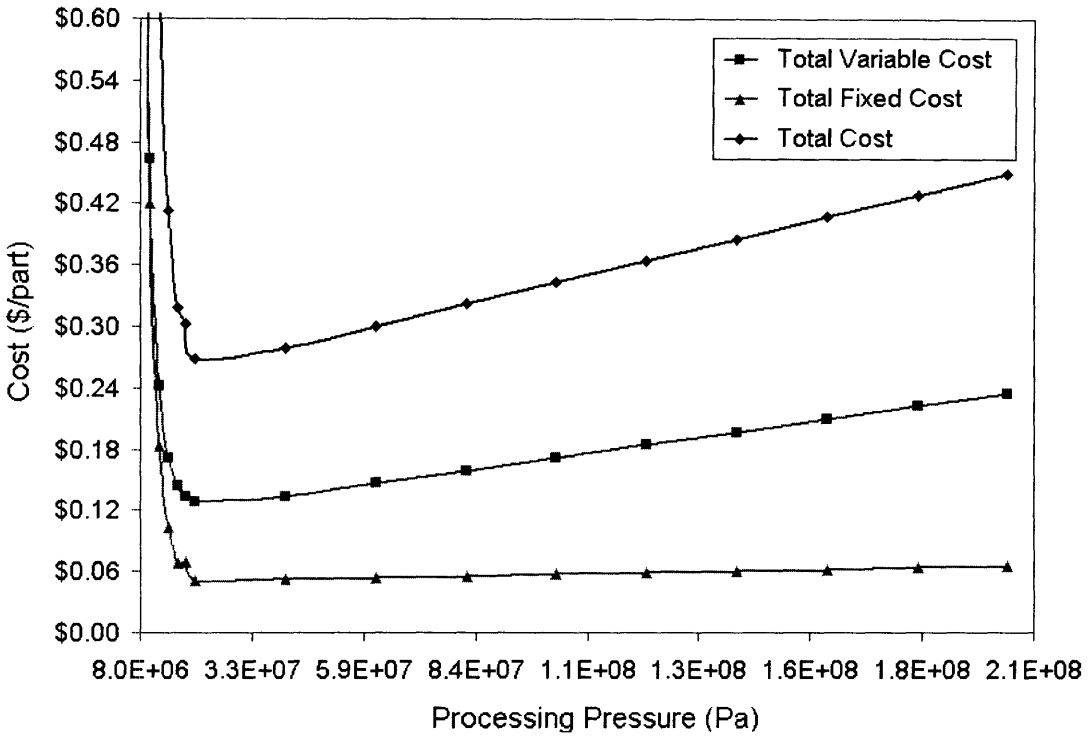

Figure 4.3 Variable, fixed and total cost per part for baroplastics as a function of processing pressure.

Because of the apparent trade-off that exists between cycle time and material costs, further analysis was conducted to determine how the cost per part varied as a function of the part weight. The results can be seen in Figure 4.4.

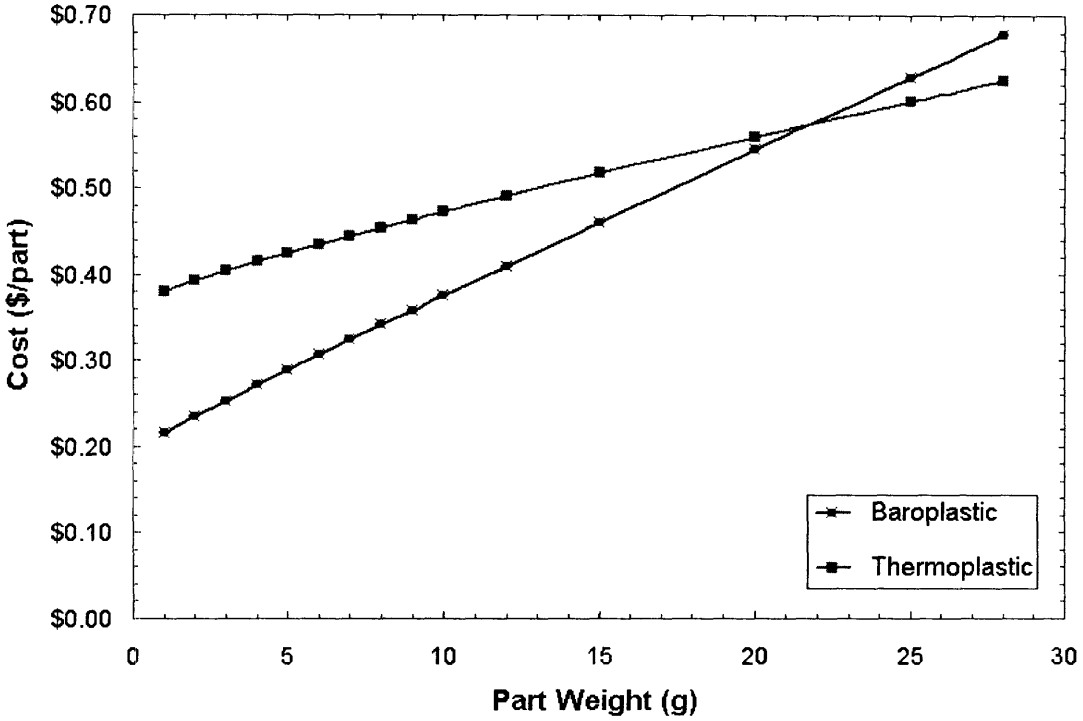

Figure 4.4 Total cost per part as a function of the part weight for baroplastic and thermoplastic processing assuming a baroplastic materials cost of $0.009/g.

For low part weights, using baroplastics will result in lower production costs, primarily because cycle times are much lower. As the part weight increases, the effect of the high material costs associated with baroplastics outweighs the effect of lower cycle times. At around a part weight of 22 g, the two cost lines meet. Above that point, it is no longer economically advantageous to use baroplastics, given the conservative materials cost estimate. This result is based on what is likely a greatly inflated materials cost. However, numerous products currently made using TPEs fall below the "critical" part weight mentioned above. Some examples mentioned earlier include gaskets, valves, stoppers, wrist bands, push buttons, etc.

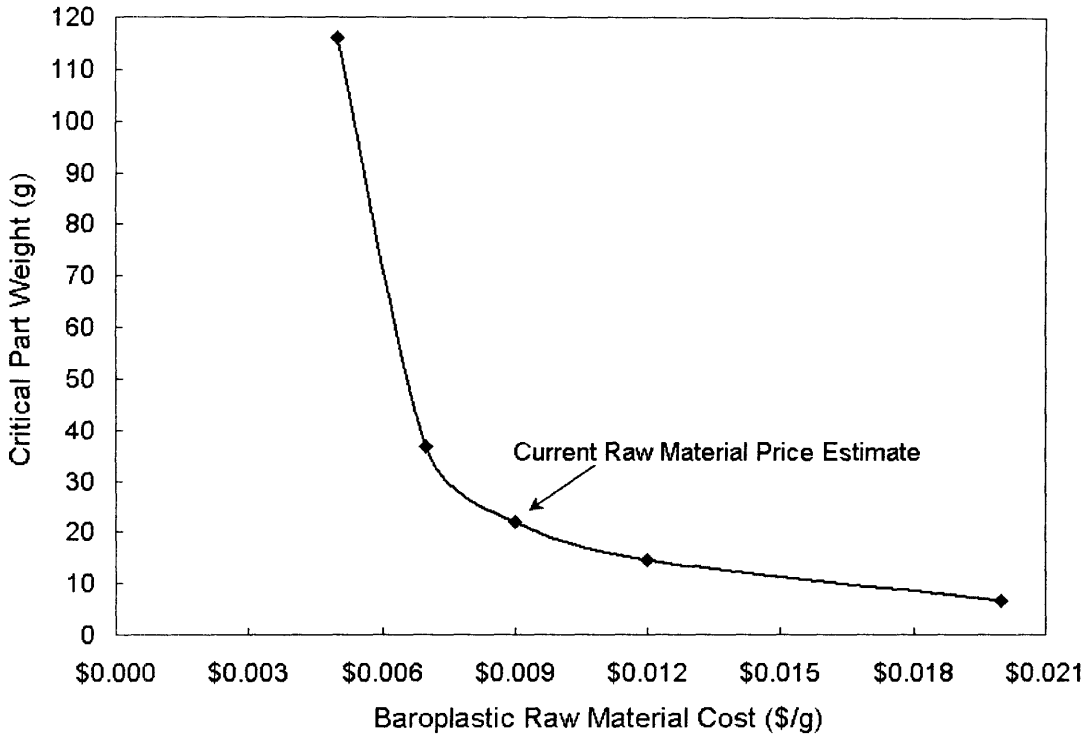

Figure 4.5 Critical part weight as a function of the baroplastic raw material cost.

The estimated material cost of baroplastics is also expected to decrease as synthesis is scaled to commercial production levels. As seen in Figure 4.5, this will have the effect of raising the "critical" part weight and expanding the potential applications of baroplastics. For example, if baroplastics cost twice as much as TPEs, the critical weight would increase to around 47 g. In fact, below a materials cost of around $0.008, the critical part weight increases substantially for only a small differential in the materials cost. If the cost of baroplastic materials was equivalent to, or less than, the cost of TPEs, there would no longer be a critical part weight. Parts fabricated using baroplastics would have a lower predicted cost than parts fabricated using TPEs regardless of their weight.

5.0 Conclusion

In conclusion, baroplastics have demonstrated their potential to be a very exciting prospect in the field of plastics manufacturing and processing. As alternatives to traditional TPEs, preliminary cost models have shown their potential to be cheaper and more environmentally friendly. However, more research still needs to be done, and in particular, the raw material cost of baroplastics must be decreased to make it economically viable for use on larger products.

One patent on baroplastic materials covering the block copolymeric structures has been issued and another patent covering the core-shell nanoparticles has been filed. This provides the essential intellectual property protection needed to reap economic benefit from commercializing the technology.

6.0 References

1. Gonzalez-Leon, J. A.; Ryu, S.; Hewlett, S.; Ibrahim, S.; and Mayes, A. M., *Core-Shell Polymer Nanoparticles for Baroplastic Processing*, Macromolecules, In press.
2. Freedonia Group Report, *Thermoplastic Elastomers to 2007 - Market Size, Market Share, Market Leaders, Demand Forecast and Sales*, December 2003.
3. Holden, G., Thermoplastic Elastomers 2nd edition, Hanser-Gardner Publications, Cincinnati 2004.
4. Gonzalez-Leon, J. A.; Acar, M. H.; Ryu, S.; Ruzette, A. G.; and Mayes, A. M., *Low-Temperature processing of 'baroplastics' by pressure-induced flow*, Nature, Vol. 426, pgs 424-428, November 2003.
5. RTP Company, http://www.rtpcompany.com/products/elastomer/, Accessed: 8/2/05
6. Crawford, R. J., Plastics Engineering (3rd Edition), pgs 323-326, 351-357, Butterworth-Heinemann, UK © 1998
7. Chemical Market Reporter, Volume 267, Issue No. 2, 1/10/2005.
8. Kirchain, R. (MIT Materials Systems Laboratory), Personal communication.
9. Seader, J. D., and E.J. Henley, Separations Process Principles, pgs 355-382, Wiley, New York, 1998
10. Matches, http://matche.com/EquipCost/, Accessed: 8/2/05
11. Mohr, M., Personal communication, MIT Course 10.32.
12. Rees, H., Mold Engineering, 2nd Edition, Hanser-Gardner Publications, Cincinnati 2005.
13. Busch, V., Technical Cost Modeling of Plastics Fabrication Processes, Ph.D Thesis, M.I.T. 1987.

Appendix A: Detailed derivation for flow of non-Newtonian polymer between 2 parallel plates

*** The folllowing analysis was modeled after an analysis outlined in Plastics Engineering, 2nd Edition by R. J. Crawford [6].*

Since polymer viscosities tend to vary depending on temperature, strain rate, stress, etc., Newtonian flow does not apply for most polymers. Non-newtonian polymer flow can be modeled using a power law relation:

$$\tau = \tau_0 \dot{\gamma}^n \tag{A.1}$$

where τ is the shear stress,τ_0 is the initial shear stress, $\dot{\gamma}$ is the strain rate, and n is the power law index. The strain rate is related to the viscosity through:

$$\frac{\eta}{\eta_0} = \left[\frac{\dot{\gamma}}{\dot{\gamma}_0}\right]^{n-1} \tag{A.2}$$

where η is the apparent viscosity, η_0 is the reference viscosity, and $\dot{\gamma}_0$ is the reference shear rate. Since the apparent viscosity is defined as the ratio of the shear stress to the shear rate, we can substitute shear rate with shear stress to obtain:

$$\frac{\eta}{\eta_0} = \left[\frac{\tau}{\tau_0}\right]^{n-1/n} \tag{A.3}$$

The power law relation then reduces to:

$$\tau = \eta\dot{\gamma} \tag{A.4}$$

Since $\dot{\gamma} = \frac{\partial V}{\partial y}$, Eqn A.4 can also be expressed as:

$$\tau = \eta\frac{\partial V}{\partial y} \tag{A.5}$$

where V is the velocity of the element.

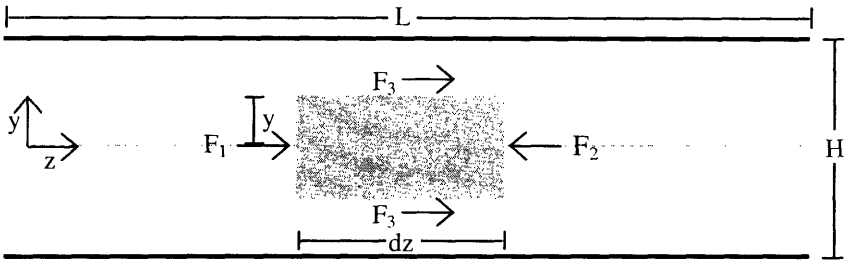

Figure A.1 Analysis of element of fluid

Figure A.1 depicts an element of fluid in the mold, where F_1, F_2, and F_3 are the shear forces acting on the element of fluid, dz is the length of the fluid element, y is the distance from the midway point of the element to any other point, H is the height of the polymer cake at any point in time during the compression, and L is the length of the part.

The three forces acting on the element of fluid can be expressed as [6]:

$$F_1 = \left(P + \frac{\partial P}{\partial z} dz \right) 2y \tag{A.6}$$

$$F_2 = 2Py \tag{A.7}$$

$$F_3 = \tau dz \tag{A.8}$$

where P is the pressure acting on the element.

For a steady flow, the forces must balance:

$$\sum F = 0 \rightarrow 2Py = \left(P + \frac{\partial P}{\partial z} dz \right) 2y - 2\tau dz \tag{A.9}$$

which reduces to:

$$\tau = y \frac{\partial P}{\partial z} \tag{A.10}$$

but Eqn A.5 still applies. By combining the two equations, we get [6]:

$$\frac{\partial V}{\partial y} = y \frac{\partial P}{\partial z} \cdot \frac{1}{\eta_0} \left[\frac{\partial V / \partial y}{\dot{\gamma}_0} \right]^{1-n} \tag{A.11}$$

Integrating this expression gives:

$$V = \left(\frac{n}{n+1}\right)\dot{\gamma}_0\left(\frac{1}{\eta_0\dot{\gamma}_0}\cdot\frac{\partial P}{\partial z}\right)^{1/n}\left[y^{(n+1)/n} - \left(\frac{H}{2}\right)^{(n+1)/n}\right] \tag{A.12}$$

The flowrate, Q, is then obtained as:

$$Q = 2W\int_0^{H/2} V dy \tag{A.13}$$

where W is the width of the channel.

When integrated, Eqn A.13, yields:

$$Q = \frac{(n+1)}{(2n+1)}WV_0H \tag{A.14}$$

where V_0 is the velocity at $y = 0$ [6]:

$$V_0 = -\left(\frac{n}{n+1}\right)\dot{\gamma}_0\left(\frac{1}{\eta_0\dot{\gamma}_0}\frac{\partial P}{\partial z}\right)^{1/n}\left(\frac{H}{2}\right)^{(n+1/n)} \tag{A.15}$$

Because the element of fluid has to move due to the pressure at the same rate that the plate moving down is displacing the element of fluid, we can write:

$$Wz\left(\frac{dH}{dt}\right) = \frac{(n+1)}{(2n+1)}WV_0H \tag{A.16}$$

Substituting the full expression for V_0, the previous expression expands to:

$$\left(\frac{n}{n+1}\right)\dot{\gamma}_0\left(\frac{1}{\eta_0\dot{\gamma}_0}\right)^{1/n}\frac{1}{z}\left(\frac{\partial P}{\partial z}\right)^{1/n} = -\left(\frac{2n+1}{n+1}\right)\frac{1}{H}\left(\frac{H}{2}\right)^{-(n+1)/n}\frac{dH}{dt} \tag{17}$$

To simplify the integration, we can define two variables:

$$S = \left(\frac{n}{n+1}\right)\dot{\gamma}_0\left(\frac{1}{\eta_0\dot{\gamma}_0}\right)^{1/n} \tag{A.18}$$

and

$$M = -\left(\frac{2n+1}{n+1}\right)\frac{1}{H}\left(\frac{H}{2}\right)^{-(n+1)/n}\frac{dH}{dt} \tag{A.19}$$

Eqn A.17 can then be written as:

$$\frac{1}{z^n}\left(\frac{\partial P}{\partial z}\right)=\left(\frac{M}{S}\right)^n \rightarrow dP=\left(\frac{M}{S}\right)^n z^n dz \tag{A.20}$$

By integrating both sides:

$$\int_0^P dP=\left(\frac{M}{S}\right)^n \int_L^z z^n dz \rightarrow P=\left(\frac{M}{S}\right)^n \frac{z^{n+1}-L^{n+1}}{n+1} \tag{A.21}$$

The force on the element, F, is:

$$F=(P)(Area)=PWdz \tag{22}$$

Substituting Eqn A.21 for P and integrating this expression gives:

$$F=\int_0^L W\left(\frac{M}{S}\right)^n \frac{z^{n+1}-L^{n+1}}{n+1}dz \rightarrow F=-\left(\frac{M}{S}\right)^n \frac{W}{n+2}L^{n+2} \tag{A.23}$$

Rearranging the equation yields:

$$M=\left(\frac{-(n+2)FS^n}{WL^{n+2}}\right)^{1/n} \tag{A.22}$$

By setting Eqn A.19 and Eqn A.22 equal, we get:

$$-\left(\frac{2n+1}{n+1}\right)\frac{1}{H}\left(\frac{H}{2}\right)^{-(n+1)/n}\frac{dH}{dt}=\left(\frac{-(n+2)FS^n}{WL^{n+2}}\right)^{1/n} \tag{A.23}$$

To simplify the integration, we again define two variables:

$$U=\left(\frac{2n+1}{n+1}\right)\left(\frac{1}{2}\right)^{-(n+1)/n} \tag{A.24}$$

and

$$T=\left(\frac{(n+2)S^n}{WL^{n+2}}\right)^{1/n} \tag{A.25}$$

Eqn A.23 can then be rewritten as:

$$UH^{\frac{-(n+1)}{n}-1}dH=TF^{1/n}dt \tag{A.26}$$

Setting the integrating limits:

$$\int_{H_0}^{H_f} UH^{\frac{-(n+1)}{n}-1} dH = \int_0^t TF^{1/n} dt \tag{A.27}$$

where H_o is the height of the polymer cake before it is compressed, and H_f is the height of the processed part after compression.

Integrating Eqn A.27, we get:

$$F = \left(\frac{U}{T} \cdot \frac{\Delta H^{n+1/n}}{n+1/n} \cdot \frac{1}{t} \right)^n \tag{A.28}$$

where

$$\Delta H = H_0 - H_f \tag{A.29}$$

By substituting for U and T and simplifying the expression further we can get a simpler form for the force equation:

$$F = B \frac{\Delta H^{-(n+1)}}{t^n} \tag{A.30}$$

where B is defined as:

$$B = \frac{2^{n+1}}{(n+2)} \left(\frac{2n+1}{n+1} \right)^n WL^{n+2} \left(\frac{\eta_0}{\dot{\gamma}_0^{n-1}} \right) \tag{A.31}$$

This is the force required to move half the polymer cake down one half the length of the channel. To get the total force for the entire cake, this value should be multiplied by 2, making the final expression:

$$F = 2B \frac{\Delta H^{-(n+1)}}{t^n} \tag{A.32}$$

Appendix B: Related Intellectual Property

Block Copolymer Baroplastics

Patent Title: Baroplastic Materials
Patent Status: Issued
Patent # 6,632,883
Date Filed: February 16th, 2001; Date Issued: October 14th, 2003
Inventors: Anne Mayes, Anne Valerie Ruzette, Thomas Russell, and Pallab Banerjee

Claims:
1. A method of processing a polymer, comprising:
providing a block copolymeric composition comprising a soft component A having a $T_{g,s}$ of less than room temperature, a hard component B in contact with the soft component A, the hard component having a $T_{g,s}$ such that hard component has negligible flow at room temperature; and applying a pressure of at least about 100 psi such that the block copolymeric composition exhibits Newtonian flow at a processing temperature that is less than 150°C., wherein the composition does not exhibit Newtonian flow at the processing temperature in the absence of said pressure.

2. A method as in claim 1, wherein components A and B of the composition are selected to have a relation $\phi_A\phi_B [(\rho_A - \rho_B)(\delta_A^2 - \delta_B^2)]$ having a positive value at a temperature above 100°C, wherein ϕ_A and ϕ_B represent volume fractions of the components A and B respectively, ρ_A and ρ_B represent reduced densities of the components A and B respectively, and δ_A and δ_B represent solubility parameters of the components A and B respectively; and the densities ρ_A and ρ_B being matched as defined by the following relationship:
$1.06\rho_A < \rho_B < 0.94\rho_A$.

3. The method of claim 2, wherein $\phi_A\phi_B [(\rho_A - \rho_B) (\delta_A^2 - \delta_B^2)]$ has a positive value at a temperature above 50°C.

4. The method of claim 2, wherein $\phi_A\phi_B [(\rho_A - \rho_B) (\delta_A^2 - \delta_B^2)]$ has a positive value at a temperature above 0°C.

5. The method of claim 1, wherein a pressure coefficient, dT/dP, of the composition has an absolute value greater than about 30°C/kbar.

6. The method of claim 5, wherein the pressure coefficient has an absolute value greater than about 50°C/kbar.

7. The method of claim 5, wherein the pressure coefficient has an absolute value greater than about 100°C/kbar.

8. The method of claim 1, wherein upon the application of pressure of at least about 100 psi and at a temperature of no more than 150°C, the composition is in a miscible state and has a glass transition temperature $T_{g,mix}$, as defined by the relation:

$$1/T_{g,mix} = w_s /T_{g,s} + w_h /T_{g,s}$$

wherein w_s and w_h are weight fractions of the soft and hard components respectively.

9. The method of claim 8, wherein the block copolymeric composition is selected from the group consisting of polystyrene-b-poly(hexyl methacrylate) copolymers wherein $0<w_s\leq 45\%$, poly(ethyl methacrylate)-b-poly(ethyl acrylate) copolymers wherein $0<w_{EMA}\leq 85\%$, polycaprolactone-b-poly(ethyl acrylate) wherein $0<w_{PCL}<100\%$, polycaprolactone-block-poly(ethyl methacrylate) wherein $0<w_{EMA}\leq 92\%$, poly(caprolactone)-block-poly(methyl methacrylate) wherein $0<w_{MMA}\leq 75\%$, poly(methyl methacrylate)-b-poly(ethyl acrylate) copolymers wherein $0<w_{MMA}\leq 65\%$, poly(ethyl methacrylate)-b-poly(methyl acrylate) copolymers wherein $0<w_{EMA}\leq 85\%$, polystyrene-block-poly(vinyl ethyl ether) wherein $0<w_{sTY}\leq 80\%$, polystyrene-block-poly(butyl acrylate) wherein $0<w_{sTY}\leq 80\%$, polystyrene-block-poly(hexyl acrylate) wherein $0<w_s\leq 80\%$, poly(propyl methacrylate)-block-poly(ethyl acrylate) wherein $0<w_{PPMA}<100\%$, poly(butyl methacrylate)-block-poly(butyl acrylate) wherein $0<w_{PBMA}<100\%$, poly(propyl methacrylate)-block-poly(propyl acrylate) wherein $0<w_{PPMA}<100\%$, poly(propyl methacrylate)-block-poly(butyl acrylate) wherein $0<w_{PPMA}<100\%$, poly(ethyl methacrylate)-block-poly(propyl acrylate) wherein $0<w_{EMA}\leq 90\%$, poly(ethyl methacrylate)-block-poly(butyl acrylate) wherein $0<w_{EMA}\leq 90\%$ poly(cyclohexyl methacrylate)-block-poly(propyl acrylate) wherein $0<w_{CHMA}\leq 80\%$, poly(cyclohexyl methacrylate)-block-poly(butyl acrylate) wherein $0<w_{CHMA}\leq 85\%$, poly(propyl acrylate)-block-poly(butyl methacrylate) wherein $0<w_{PPA}<100\%$, and poly(propyl acrylate)-block-polycaprolactone wherein $0<w_{PPA}<100\%$.

10. The method of claim 9, wherein poly(butyl acrylate) is substituted by a random copolymer of two or more monomers selected from MA, EA, PA, HA, OA, DA, and LA.

11. The method of claim 9, wherein poly(ethyl acrylate) is substituted by a random copolymer of two or more monomers selected from MA, PA, BA, HA, OA, DA, and LA.

12. The method of claim 9, wherein poly(propyl acrylate) is substituted by a random copolymer of two or more monomers selected from MA, EA, BA, HA, OA, DA, and LA.

13. The method of claim 9, wherein poly(butyl methacrylate) is substituted by a random copolymer of two or more monomers selected from MMA, EMA, PMA, HMA, OMA, DMA, and LMA.

14. The method of claim 9, wherein poly(ethyl methacrylate) is substituted by a random copolymer of two or more monomers selected from MMA, PMA, BMA, OMA, HMA, DMA, and LMA.

15. The method of claim 9, wherein poly(propyl methacrylate) is substituted by a random copolymer of two or more monomers selected from MMA, EMA, BMA, OMA, HMA, DMA, and LMA.

16. The method of claim 9, wherein polystyrene is substituted by a random copolymer comprising any of the following combinations: BMA/CHMA, S/BMA, S/CHMA, S/BMA/CHMA.

17. The method of claim 8, wherein the hard block has a T_g of less than about 80°C.

18. The method of claim 8, wherein the hard block has a T_g of less than about 50°C.

19. A pressure sensitive adhesive formed by the method of claim 1.

20. A pressure molded or injection molded article formed by the method of claim 1.

21. An elastomer formed by the method of claim 1.

22. A block copolymer comprising:
a soft block having a $T_{g,s}$ of less than room temperature;

a hard block bonded to the soft block, the hard block having a $T_{g,s}$ such that the hard block has negligible flow at room temperature; and
wherein a pressure coefficient that favors miscibility, defined as a change in temperature of the disorder-order transition, T_{DOT}, of the block copolymer, as a function of change in pressure, $P(dT_{DOT}/dP)$, of the block copolymer has an absolute value greater than about 30°C/kbar.

23. The block copolymer of claim 22, wherein the pressure coefficient has an absolute value greater than about 50°C/kbar.

24. The block copolymer of claim 22, wherein the pressure coefficient has an absolute value greater than about 100°C/kbar.

25. The block copolymer of claim 22, wherein at a temperature of no more than 150°C and under the application of pressure of at least 100 psi, the block copolymer is in a miscible state and has a glass transition temperature $T_{g,mix}$, as defined by the relation:

$$1/T_{g,mix} = w_s /T_{g,s} + w_h /T_{g,s}$$

wherein w_s and w_h are weight fractions of the soft and hard blocks respectively.

26. The block copolymer of claim 25, wherein the block copolymer is in a miscible state at a temperature of no more than 100°C under the application of pressure of at least 100 psi.

27. The block copolymer of claim 25, wherein the block copolymer is in a miscible state at a temperature of no more than 60°C under the application of pressure of at least 100 psi.

28. A method as in claim 1, comprising applying a pressure of at least about 200 psi such that the block copolymeric composition exhibits Newtonian flow at a processing temperature that is less than 150°C, wherein the composition does not exhibit Newtonian flow at the processing temperature in the absence of said pressure.

29. A method as in claim 28, wherein the pressure is at least about 500 psi.

30. A method as in claim 28, wherein the pressure is at least about 1000 psi.

31. A block copolymer as in claim 22, wherein, upon applying a pressure of at least about 200 psi, the block polymer exhibits Newtonian flow at a processing temperature that is less than 150°C, and the block copolymer does not exhibit Newtonian flow at the processing temperature in the absence

of said pressure.

32. A block copolymer as in claim 31, wherein the pressure is at least about 500 psi.

33. A block copolymer as in claim 31, wherein the pressure is at least about 1000 psi.

Core-Shell Nanoparticle Baroplastics

Patent Title: Structured Baroplastic Materials
Patent Status: Pending
Application # 60/438,445
Date Filed: January 7th, 2003
Inventors: Anne M. Mayes, Sang Woog Ryu, Metin Acar, and Juan Gonzalez

Claims

1. A method, comprising:
providing a solid article comprising a first material and a second material in nanoscale proximity with each other; and
applying pressure to the article sufficient to cause at least a portion of the article to exhibit fluidity at a temperature at which, in the absence of the pressure, the portion of the article does not exhibit fluidity.

2. The method of claim 1, wherein the first material and the second material are not covalently bound to each other.

3. The method of claim 1, wherein the pressure is at least about 100 psi.

4. The method of claim 3, wherein the pressure is at least about 500 psi.

5. The method of claim 4, wherein the pressure is at least about 1000 psi.

6. The method of claim 5, wherein the pressure is at least about 5000 psi.

7. The method of claim 1, wherein the first material and the second material are miscible at a pressure of at least about 100 psi.

8. The method of claim 1, wherein the first material and the second material, when mixed, have an average glass transition temperature of less than about 25 °C at a pressure of at least about 100 psi.

9. The method of claim 1, wherein the first material exhibits fluidity at a pressure of at least about 100 psi.

10. The method of claim 1, wherein the article is a film.

11. The method of claim 1, wherein the article is a particle.

12. The method of claim 11, wherein the particle has a maximum dimension of less than about 1 micrometer.

13. The method of claim 12, wherein the particle has a maximum dimension of less than about 100 nm.

14. The method of claim 13, wherein the particle has a maximum dimension of less than about 10 nm.

15. The method of claim 11, wherein the particle includes a core region comprising the first material and a shell region comprising the second material.

16. The method of claim 15, wherein the core region has a glass transition temperature less than about 25 °C.

17. The method of claim 15, wherein the shell region has a glass transition temperature of at least about 25 °C.

18. The method of claim 1, wherein the first material comprises a first polymer and the second material comprises a second polymer.

19. The method of claim 18, wherein the first polymer and the second polymer are selected from a group of:

polystyrene and poly(2-ethyl hexyl acrylate), polystyrene and poly(butyl acrylate), poly(ethyl acrylate) and poly(ethyl methacrylate), polystyrene and poly(hexyl methacrylate), polystyrene and poly(lauryl acrylate-r-methyl acrylate), poly(ethyl methacrylate) and poly(ethyl acrylate), poly(caprolactone) and poly(ethyl acrylate), poly(caprolactone) and poly(ethyl methacrylate), poly(methyl methacrylate) and poly(ethyl acrylate), poly(ethyl methacrylate) and poly(methyl acrylate), polystyrene and poly(vinyl ethyl ether), polystyrene and poly(phenyl methyl siloxane), polystyrene and poly(butyl acrylate), polystyrene and poly(hexyl acrylate), polystyrene and poly(2-ethyl hexyl acrylate), poly(propyl methacrylate) and poly(ethyl acrylate), poly(butyl methacrylate) and poly(butyl acrylate), poly(propyl methacrylate) and poly(propyl acrylate), poly(propyl methacrylate) and poly(butyl acrylate), poly(ethyl methacrylate) and poly(propyl acrylate), poly(ethyl methacrylate) and poly(butyl acrylate), poly(cyclohexyl methacrylate) and poly(propyl acrylate), poly(cyclohexyl methacrylate) and poly(butyl acrylate), poly(propyl acrylate) and poly(butyl methacrylate), and poly(propyl acrylate) and poly(caprolactone).

20. The method of claim 19, wherein the first polymer and the second polymer are selected from a group of:

polystyrene and poly(hexyl methacrylate) at $0 < w_{PS} \leq 45\%$,
poly(ethyl methacrylate) and poly(ethyl acrylate) at $0 < w_{PEMA} \leq 85\%$,
polycaprolactone and poly(ethyl acrylate) at $0 < w_{PCL} < 100\%$,
poly(caprolactone) and poly(ethyl methacrylate) at $0 < w_{PEMA} \leq 92\%$,
poly(methyl methacrylate) and poly(ethyl acrylate) at $0 < w_{PMMA} \leq 65\%$,
poly(ethyl methacrylate) and poly(methyl acrylate) at $0 < w_{PEMA} \leq 85\%$,
polystyrene and poly(vinyl ethyl ether) at $0 < w_{PS} \leq 80\%$,
polystyrene and poly(phenyl methyl siloxane) at $0 < w_{PS} \leq 75\%$,
polystyrene and poly(butyl acrylate) at $0 < w_{PS} \leq 80\%$,
polystyrene and poly(hexyl acrylate) at $0 < w_{PS} \leq 80\%$,
polystyrene and poly(2-ethyl hexyl acrylate) at $0 < w_{PS} \leq 80\%$,

poly(propyl methacrylate) and poly(ethyl acrylate) at $0 < w_{PPMA} < 100\%$,
poly(butyl methacrylate) and poly(butyl acrylate) at $0 < w_{PBMA} < 100\%$,
poly(propyl methacrylate) and poly(propyl acrylate) at $0 < w_{PPMA} < 100\%$,
poly(propyl methacrylate) and poly(butyl acrylate) at $0 < w_{PPMA} < 100\%$,
poly(ethyl methacrylate) and poly(propyl acrylate) at $0 < w_{EMA} \leq 90\%$,
poly(ethyl methacrylate) and poly(butyl acrylate) at $0 < w_{EMA} \leq 90\%$,
poly(cyclohexyl methacrylate) and poly(propyl acrylate) at $0 < w_{CHMA} \leq 80\%$,
poly(cyclohexyl methacrylate) and poly(butyl acrylate) at $0 < w_{CHMA} \leq 85\%$,
poly(propyl acrylate) and poly(butyl methacrylate) at $0 < w_{PPA} < 100\%$, and
poly(propyl acrylate) and poly(caprolactone) at $0 < w_{PPA} < 100\%$.

21. The method of claim 1, further comprising placing the article in a mold.

22. The method of claim 1, further comprising extruding the article.

23. The method of claim 1, further comprising removing the pressure from the article.

24. The method of claim 1, wherein the fluidity is Newtonian.

25. An article, comprising:

a first material and a second material in nanoscale proximity with each other, wherein the first material and the second material are immiscible at ambient pressure, and miscible at a pressure of at least about 100 psi at a temperature at which, in the absence of the pressure, the first material and the second material are immiscible.

26. The article of claim 25, wherein the first material and the second material are not covalently bound to each other.

27. An article, comprising:

a first material and a second material in nanoscale proximity with each other, wherein the first material is solid at ambient pressure and exhibits fluidity at pressures of at least about 100 psi at a temperature at which, in the absence of the pressure, the first material does not exhibit fluidity.

28. The article of claim 27, wherein the first material and the second material are not covalently bound to each other.

29. An article, comprising:

a baroplastic material formed from a composition having a first material and a second material in nanoscale proximity with each other, wherein the first material and the second material are not covalently bound to each other.

30. The article of claim 29, wherein the composition is a particle.

31. The article of claim 29, wherein the particle includes a core region comprising the first material and a shell region comprising the second material.

32. A method, comprising:

providing an article comprising a first material and a second material defining an interfacial area therebetween of at least about 20 m^2/g, and

applying pressure to the article sufficient to cause at least a portion of the article to exhibit fluidity at a temperature at which, in the absence of the pressure, the portion of the article does not exhibit fluidity.

33. The article of claim 32, wherein the first material and the second material are not covalently bound to each other.

34. An article, comprising:

a first material and a second material defining an interfacial area therebetween of at least about 20 m^2/g, wherein the first material and the second material are immiscible at ambient pressure, and miscible at a pressure of at least about 100 psi at a temperature at which, in the absence of the pressure, the first material and the second material are immiscible.

35. The article of claim 34, wherein the first material and the second material are not covalently bound to each other.

36. An article, comprising:

a first material and a second material defining an interfacial area therebetween of at least about 20 m^2/g, wherein the first material is solid at ambient pressure and exhibits fluidity at pressures of at least about 100 psi at a temperature at which, in the absence of the pressure, the first material does not exhibit fluidity.

37. The article of claim 36, wherein the first material and the second material are not covalently bound to each other.

38. An article, comprising:

a baroplastic material formed from a composition having a first material and a second material defining an interfacial area therebetween of at least about 20 m^2/g, wherein the first material and the second material are not covalently bound to each other.

39. A method, comprising:

providing a first solid polymeric article and a second solid polymeric article; and

applying pressure to the first and second solid polymeric articles sufficient to allow the solid polymeric articles to fluidize and intermix.

40. A method, comprising:

producing a polymer from a particulate precursor having an initial polydispersity index; and

recycling the polymer at least three times while maintaining the polydispersity index of the polymer to within about 95% of the initial polydispersity index.

41. A method, comprising:

producing a polymer from a particulate precursor having an initial concentration of impurities; and

recycling the polymer at least three times while maintaining the concentration of impurities of the polymer to within about 95% of the initial concentration of impurities.

42. A method, comprising:

producing a polymer from a particulate precursor having an initial average molecular weight; and

recycling the polymer at least three times while maintaining the average molecular weight of the polymer to within about 95% of the initial average molecular weight.

43. A method comprising:

processing a particular polymeric article, meeting industry standards for that article, from a polymer precursor material; and

recycling the polymeric article at least three times while maintaining physical and chemical characteristics of the article sufficient to meet industry standards for the particular article.

Appendix C: Methanol/Water Distillation Column

*** The folllowing analysis was modeled after an analysis outlined in Separations Process Principles by Seader, J. D., and E.J. Henley [9].*

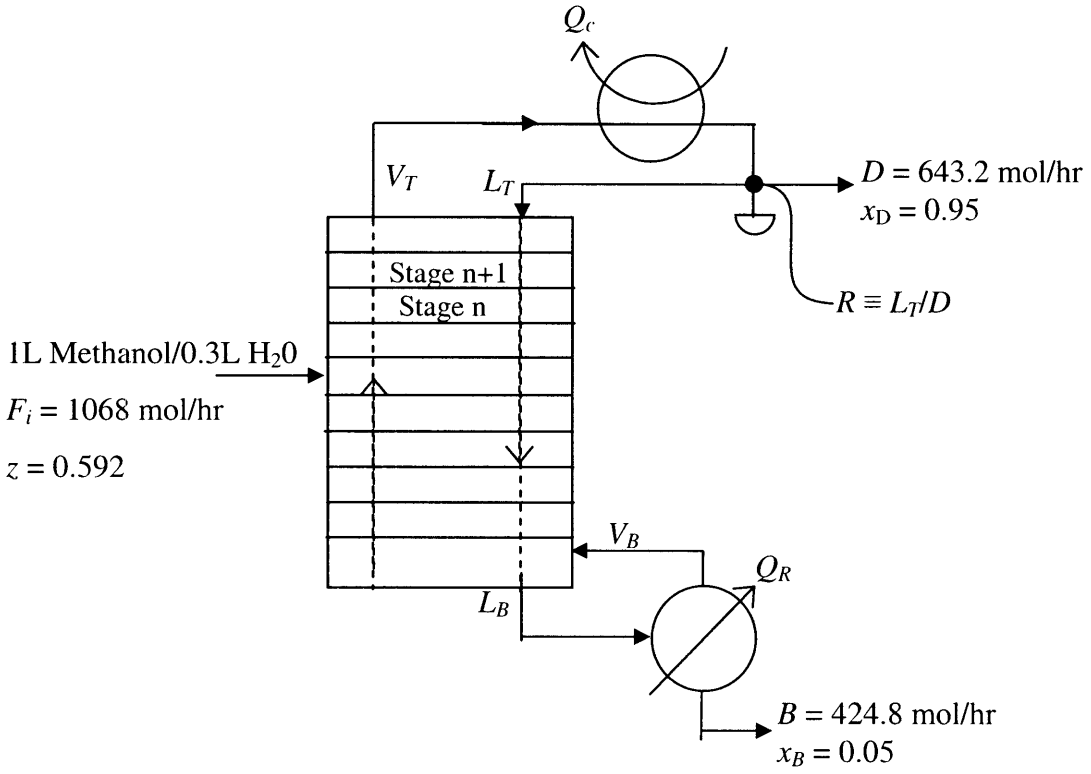

Figure C.1 Diagram of distillation column for methanol/water separation

The distillation column was designed to separate the methanol/water waste stream resulting from the synthesis of 2000 kg of PS/PBA core-shell polymer. If the synthesis is assumed to be a continuous process operating for 240 days/yr and 8 hrs/day, the stream entering the distillation column is 26.15 L/hr of methanol mixed with 7.85 L/hr of water. This is equivalent to 632 mol/hr of methanol and 436 mol/hr of water for a total of 1068 mol/hr entering the column as feed, F_i. The mole fraction of the more volatile component in the feed, methanol, can be calculated as [9]:

$$z = \frac{\text{Mole fraction of more volatile component}}{\text{Total \# of moles in feed}} \qquad \text{(C.1)}$$

Since methanol is the more volatile component it will evaporate and rise to the top of the tower where a condenser will cool it down to a liquid. A portion of the condensed liquid will be recycled back into the column based on the reflux ratio chosen. The remaining purified liquid methanol, D_o, will be collected and recycled. The purity of the methanol being recycled was chosen to be 95%. Therefore, the mole fraction of methanol in the D_o stream, x_D, is 0.95. To maintain the mass balance, the mole fraction of methanol, x_B, in the purified water stream, B_o, must be 0.05. As the purity increases, more stages are required in the distillation column and costs increase. We can then perform mass and mole balances on the entire column to determine the values of D_o and B_o [9]:

$$z \times F_i = x_B B_o + x_D D_o \tag{C.2}$$

$$F_i = B_o + D_o \tag{C.3}$$

By solving the system of equations, we find that D_o = 643.2 mol/hr and B_o = 424.8 mol/hr.

An important parameter in distillation is the relative volatility, α, of the two components being separated. For a methanol/water system, the relative volatility has been reported to be 3.27 [9].

The reflux ratio, R, is defined as the ratio of the liquid that is recycled back into the distillation column, L_T (where the subscript, T, refers to the *top* of the column), to the purified methanol stream that is collected [9]:

$$R \equiv \frac{L_T}{D_o} \tag{C.4}$$

The minimum reflux ratio, R_{min}, required can be calculated as:

$$R_{\min} = \frac{1}{z(\alpha - 1)} \tag{C.5}$$

However, the actual value of the reflux ratio used industrially is given by:

$$R = 1.3 R_{\min} \tag{C.6}$$

In order to determine the number of stages required for the distillation, flash calculations must be iteratively performed to satisfy phase equilibrium criteria:

$$x_n = \frac{y_n}{\alpha - (\alpha - 1) y_n} \tag{C.7}$$

where x_n is the mole fraction of the more volatile component in the liquid phase and y_n is the mole fraction of the more volatile component in the vapor phase.

In addition to Eqn C.7, two mass balances must also be performed. The first mass balance is on the top half of the distillation column as:

$$\text{MB}_{\text{TOP}}: y_{n+1} = \frac{L_T}{V_T} x_n + \frac{D}{V_T} x_D \tag{C.8}$$

where V_T is the molar flow rate of vapor rising to the top of the column and the subscripts n and $n+1$ denote two adjacent stages.

Since $V_T = L_T + D_o$, and given the definition of R in Eqn C.4, Eqn C.8 can be rewritten as [9]:

$$y_{n+1} = \frac{R}{R+1} x_n + \frac{1}{R+1} x_D \tag{C.9}$$

Similarly, a mass balance can be performed on the bottom half of the column as:

$$\text{MB}_{\text{BOT}}: y_{n+1} = \frac{\bar{L}}{\bar{V}} x_n + \frac{B}{\bar{V}} x_B \tag{C.10}$$

where $\bar{L}$ and $\bar{V}$ are the total molar flows of liquid and vapor respectively in the column. By definition:

$$\bar{L} = \bar{V} + B_o \tag{C.11}$$

$$\frac{B_o}{\bar{V}} = \frac{1}{V_B} \tag{C.12}$$

where V_B is the boilup ratio and can be determined using:

$$V_B = D_o\left(R+1-{}^{F_i}\!/_{D_o}\right) \tag{C.13}$$

Substituting Eqns. C.11 and C.12 into Eqn C.13, it can be rewritten as [9]:

$$y_{n+1} = \frac{V_B+1}{V_B}x_n - \frac{1}{V_B}x_B \tag{C.14}$$

With all the relevant parameters identified, an iterative process can be performed to determine how many stages are required to purify the mixture to the desired level. Table C.1 shows the mole fractions of methanol in the vapor and liquid phase in each stage. The first value of y_n was set to 0.95, the desired purity of the distillate. The value of x_n for each stage was calculated using Eqn C.7 and the value of vapor mole fraction of methanol in the next stage, y_{n+1}, was calculated using either Eqn C.9 or Eqn C.14. The switch to using the bottom mass balance, shown in Eqn C.14, was made when the liquid mole fraction crossed the feed value of 0.592.

Table C.1 Iterative table used to determine the required number of stages in the distillation column

Stage	y	x	
1	0.95	0.853	← using MB_{TOP}
2	0.902	0.738	
3	0.845	0.626	
4	0.629	0.342	← switched over
5	0.344	0.138	to MB_{BOT}
6	0.139	0.047	

It can be seen that in order to achieve a purity of 95% methanol in the distillate and 5% in the bottoms, 6 stages of distillation will be needed. In order to cost a six stage distillation column, a capital equipment costing website was used [10]. If a two-foot spacing between each stage is assumed, the cost of the column was determined to be roughly $6500. The amortized cost of the column over 15 years assuming a 10% capital recovery rate is around $855/yr.

Finally, energy costs associated with the reboiler and condenser were calculated. An energy balance for a total condenser yields:

$$\text{Condenser: } Q_C = D_o(R+1)\Delta H_{vap} \tag{C.15}$$

where Q_C is the heat removed from the condenser, and ΔH_{vap} is the average molar heat of vaporization of the two components (39.2 kJ/mol).

Similarly, an energy balance for the reboiler yields:

$$\text{Reboiler: } Q_R = Q_C\left(\frac{BV_B}{D_o(R+1)}\right) \tag{C.16}$$

where Q_R is the heat requirement of the reboiler.

Using the calculated heat requirements in the condenser and reboiler, the steam rate, m_s, and cooling water rate, m_{cw}, can be calculated as:

$$m_s = \frac{MW_{steam}Q_R}{\Delta H_{vap}^{steam}} \tag{C.17}$$

$$m_{cw} = \frac{Q_C}{C_{P_{H_2O}}\Delta T} \tag{C.18}$$

where MW_{steam} is the molecular weight of steam, ΔH_{vap}^{steam} is the heat of vaporization of steam, $C_{P_{H_2O}}$ is the specific heat of water (0.0752 kJ/mol·K), ΔT is the difference between the temperature at which the steam exits and enters the condenser.

Using Eqns C.17 and C.18, the required steam rate for the reboiler is 20.8 kg/hr and the required cooling water rate, assuming a standard ΔT of 5°C, is 132 kmol/hr. Given that the cost of cooling water is \$0.00015/gal [11] and the cost of steam \$0.0036/lb [11], the total energy cost associated with the distillation column is around \$500/yr.

The total cost of methanol is then the initial cost of purchasing 1L of methanol in addition to 0.05 L/hr to replenish the methanol that is not separated from the water. At a cost of $0.238/L, the total cost of methanol required is around $123/yr. The total annual cost of running the distillation column can then be estimated at $1,478/yr. For an annual production volume of 2000 kg of core-shell baroplastic, the total cost of methanol is $0.000739 per gram of core-shell baroplastic synthesized. This is an order of magnitude less than the cost of methanol without recycling as seen in Table 4.1 ($0.00594 per gram of core-shell baroplastic synthesized).

Appendix D: Detailed Excel spreadsheet for Baroplastics cost model

The cost model takes as inputs information on the material that will be processed, the final part that will be made, processing conditions, machine, labor and plant data, energy inputs, and production levels, and outputs an expected cost per part. The tables below contain the values for each input that were gathered from published data, calculated, or approximated. Below each table, any equations that were used to calculate a value are described.

Table D.1 shows the baroplastic material that will be used and its relevant mechanical and material properties. The part weight and dimensions and the processing conditions are defined.

Table D. 1 Summary of part and material inputs to model for baroplastic materials

PART/MATERIAL INPUTS		
Material	Core-shell nanoparticle (PS/PBA)	
% Polystyrene	51 00	
Nanoparticle size (nm)	72 20	
Apparent viscosity (Pa·sec)	1760185 769	
Power Law index	0 18	
Density (g/cm^3)	1	Assumed
Heat Capacity (J/kg·K)	0.34	Assumed (Heat capacity of PS)
Thermal Conductivity (W/m·K)	0.13	
Weight of part (g)	1.70	
Pellet length (m)	0 040	must be < part length
Pellet width (m)	0 070	
Pellet thickness (m)	0.002625	
Part length (m)	0.07	Part length + height of sides
Part width (m)	0 07	Part width + height of sides
Part thickness (m)	0 0015	
Melting Temperature (°C)	25	
Tool Temperature (°C)	25	
Ejection Temperature (°C)	25	
Processing force (N)	100000 00	
Processing Pressure (Pa)	20408163.27	
Processing temperature (°C)	25	

Once the pellet's length and width are inputted, the pellet height, H_{PE} (m), is automatically calculated by assuming volume conservation:

$$H_{PE} = \frac{V_{PA}}{L_{PE} \times W_{PE}} \tag{D.1}$$

where V_{PA} is the part volume, L_{PE} is the pellet length (m), and W_{PE} is the pellet width (m). The processing pressure, P (Pa), is calculated as:

$$P = \frac{F}{L_{PA} \times W_{PA}} \tag{D.2}$$

where F is the processing force (N), L_{PA} is the part length (m), and W_{PA} is the part width (m).

Table D.2 contains exogenous data like market information, desired production levels, and production times. It also contains data on the capital recovery rate, building space, machine and energy prices, labor space requirements, etc.

Table D.2 Summary of exogenous data inputs to model for baroplastic materials

EXOGENOUS DATA			
Total Market Share	50000	(000/yr)	
Expected % Market Share	2.00%		Changing this will updated the
Annual Production Volume	1000	(000/yr)	Annual PV automatically
Facility Production Capacity	3,000	(000/yr)	
Product Life	5	yrs	Estimated value
Direct Wages (w/ benefits)	$15.00	/hr	
Working Days/Yr	240		
Downtimes			
No Operations	7	hrs/day	Machine running from 8am - 8pm
Planned Paid	1	hrs/day	Setup is 2 hours
Planned Unpaid	1.2	hrs/day	
Capital Recovery Rate	10%		
Price to Rent, Building Space per Year	$30	/m^2	Value
Price of Electricity	$0.050	/kWh	Average US value, Source: DOE
Accounting Life of Machine	15	yrs	Estimated value
Overhead Burden (% fixed costs)	31.2%		
Cost per machine	$67,890	/machine	
Space Required per machine	30	m^2/machine	
Office Space for Indirect Workers	40	m^2/worker	

The annual production volume, PV (parts/yr), is calculated based on inputted market share information:

$$PV = EMS \times MS \tag{D.3}$$

where EMS is the percent expected market share (%/yr), and MS is the total market share (parts/yr).

The correlations shown in Eqn D.4 and Eqn D.5 used to calculate the press machine cost, C_{MC} ($), and space required per machine, S_{MC} (m^2), were obtained from the Materials System Laboratory (MSL) at MIT [8]:

$$C_{MC} = 61540 + 562.5 \times 0.000112 \times F + 0.114[(1000 \times L_{PA} + 150) + (1000 \times W_{PA} + 150)] \quad \text{(D.4)}$$

$$S_{MC} = 30 + 0.0203F \quad \text{(D.5)}$$

Table D.3 contains information related to the processing aspects including scrap and reject rates, mold costs and lifetime, and energy requirements.

Table D.3 Summary of process inputs to model for baroplastic materials

PROCESS INPUTS			
Unplanned Downtime	1.50	hrs/day	Estimate
Material Scrap Rate	2.0%		
Reject Rate	10.0%		
Direct Laborers Per Machine	1		
Indirect workers	3		
Dedicated Equipment (1/0)	1	(1=y;0=n)	
Number of Cavities in mold	10		
Auxiliary Equip. Cost (% mmch)	20.0%		
Installation Cost (% mmch)	20.0%		
Maintenance Cost (% invc)	5.0%		
Mold Cost	$6,421.0		
Tool Actions (1/0)	0	(1=y;0=n)	
Annual Tooling Cost	$2,500.00	/year	
Baseline Mold Life	1,500,000	cycles	
Avg Compression Power Consumption	560	kWh	
Avg Heating Energy Consumption	0.000	kWh	
Avg Refrigeration Needed for Cooling	0.000	kWh	based on 3.516 kW/ton refrigeration
Amount of Cooling Water Required	0.000	gal/hr	ΔT_c = 5°C
Cost of Refrigeration	$2.46	/ton	
Cost of Cooling Water	$0.00015	/gal	

The correlation used to calculate the cost of the mold, C_{MD} ($), was also obtained from the MSL [8]. The part dimensions, projected dimensions, and weight in the correlation must be multiplied by the number of cavities in the mold:

$$C_{MD} = 48280\left(\frac{SA_{PA}}{PSA_{PA}}\right)^{1.08}[2.2 \times PW]^{0.6} \quad \text{(D.6)}$$

where SA_{PA} is the surface area of the part (m^2), PSA_{PA} is the projected surface area of the part (m^2), and PW is the part weight (g).

Another correlation obtained from the MSL determines how much power is required to apply the compressive force, *Po* (kwh), needed on the parts:

$$Po = 0.203 \times F \times \frac{3600}{TCT} \tag{D.7}$$

where *TCT* is the total cycle time (sec/part).

The average amount of energy required to heat the mold, *HE* (kwh), to the desired temperature was calculated using [12]:

$$HE = \frac{1}{E}\left[PW \times \frac{3600}{TCT} \times C_P \times 4.187 \times (T_P - T_R) \right] / 3{,}600{,}000 \tag{D.8}$$

where E is the efficiency of heating and cooling and a function of the material the mold is constructed from, C_P is the heat capacity of the material being molded (J/kg·K), T_P is the processing temperature (°C), and T_R is room temperature (°C).

The average amount of refrigeration energy, *CE* (kwh), needed to cool the mold back to the ejection temperature was calculated using [12]:

$$CE = \frac{1}{E}\left[PW \times \frac{3600}{TCT} \times C_P \times 4.187 \times (T_P - T_E) \right] / (3{,}600{,}000 \times 3.615) \tag{D.9}$$

where T_E is the ejection temperature (°C).

The average amount of cooling water, *CW* is the average amount of cooling water needed (gal/hr), needed to provide the cooling energy was calculated using [12]:

$$CW = \frac{1}{E}\left[PW \times \frac{3600}{TCT} \times C_P \times 4.187 \times (T_P - T_R) \right] / (5 \times 4.187 \times 1000) \tag{D.10}$$

Table D.4 contains information on the material requirements for the process.

Table D.4 Summary of material requirement inputs to model for baroplastic materials

Material Requirements:	
Raw Material Price	9.00 $/kg
Amt of material per Part	1.73 g
Annual Material Input	1,927 kg

The actual amount of material that is needed for each part, M_{PA} (g), is determined based on an estimated part scrap rate:

$$M_{PA} = PW(1 + MSR) \tag{D.11}$$

where MSR is the material scrap rate for each part (%/part).

The total amount of material needed annually, AMI (kg), can then be calculated as:

$$AMI = EPV \times M_{PA}/1000 \tag{D.12}$$

where EPV is the effective production volume (parts/yr) calculated as seen in Eqn D.13 below.

Table D.5 contains process information based on both production and capacity. In some instances, capacity values will be used to calculate process inputs while actual production values are used to calculate others. For example, the building space requirement will be based on the capacity of the plant, even though production values may be below capacity for a certain amount of time.

Table D.5 Summary of process calculation in cost model for baroplastic materials

Process Calculations		
Effective Production Volume	1,111,112	
Effective Capacity	3,333,334	
Capacity and Volume are Consistent?	1	
Available operating time per machine	3,756	hours / year
Effective Cycle Time *(from below)*	1.462	secs / part
Required Operating Time (produced)	451	hours / year
Required Operating Time (capacity)	1,354	hours / year
Run-Time for One Machine (produced)	12%	
Run-Time for One Machine (capacity)	36%	
Number of Parallel Streams	1.00	
Paid Operating Time (available in year)	3,432	hours / year
Actual Paid Operating Time (allocated)	412	person-hours / year
Number of tools required	12	
Required Building Space	150	/m^2
Annual Energy Consumption	252,622	kWh/year

The effective production volume, *EPV*, is calculated based on the percentage of parts that are rejected in each batch as seen in Eqn D.13:

$$EPV = \frac{PV}{\left(1 - RR/100\right)} \tag{D.13}$$

where *RR* is the part reject rate (%/yr).

Similarly, the effective production capacity, *EPC* (parts/yr), is also calculated based on the reject rate:

$$EPC = \frac{PC}{\left(1 - RR/100\right)} \tag{D.14}$$

where *PC* is the annual production capacity (parts/yr).

The effective cycle time, *ECT* (sec/part), for each part is calculated based on the number of cavities in each mold:

$$ECT = \frac{TCT}{N_C} \tag{D.15}$$

where N_C is the number of part cavities in the mold.

The required operating time, *ROT* (hrs/yr), is calculated based on the effective cycle time and production volume:

$$ROT = \frac{ECT}{3600} \times PV \tag{D.16}$$

The percentage of time each machine will run can then be calculated based on the amount of time each machine can operate per day:

$$RTOM = \frac{ROT}{OTM} \tag{D.17}$$

where *RTOM* is the run-time for one machine (%/yr) and *OTM* is the available operating time per machine (hrs/yr).

The total number of machines running in parallel that are needed to manufacture the desired number of parts, N_{PM}, can be calculated as:

$$N_{PM} = \text{ROUNDDOWN}(ROT + 1) \tag{D.18}$$

The total paid operating time, *POT* (hrs/yr), is then calculated as a function of the number of hours that are effectively worked:

$$POT = WD(24 - NO - PU - UD) \tag{D.19}$$

where *WD* is the number of working days per year, *NO* is the number of hours per day when no operations are taking place, *PU* is the number of planned unpaid hours per day, and *UD* is the number of unplanned downtime hours per day.

The actual paid operating time, *APOT* (person-hrs/yr), can then be calculated as:

$$APOT = POT \times RTOM \times DLM \tag{D.20}$$

where *DLM* is the number of direct laborers per machine.

The number of tools required, N_T, is calculated based on the effective production capacity and the product and mold lives:

$$N_T = EPC\frac{PL}{ML} \tag{D.21}$$

where PL is the product life (yrs) and ML is the baseline mold life (cycles).

The building space required, B_S (m^2), is calculated based on the space needed for machines and the space needed for the administrative staff's office space:

$$B_S = S_{MC} \times N_{PM} + S_{IW} \times N_{IW} \tag{D.22}$$

where S_{IW} is the office space required for indirect workers (m^2) and N_{IW} is the number of indirect workers.

Finally, the total annual energy consumption, AE (kwh/yr), associated with processing is calculated based on the hourly power consumption and the total operating time:

$$AE = ROT \times Po \tag{D.23}$$

Table D.6 is a summary of the times associated with processing.

Table D.6 Summary of cycle time calculations in cost model for baroplastic materials

Cycle Time Calculations	
Mold Coplexity Correction Factor	1.2
Heating & Cooling Time (sec)	0.0
Compression Time (sec)	14.618
Total Cycle Time (sec)	28.494
	2.11 cycles/min.
B factor	25.99

The time required for heating and cooling, HCT (sec/part), can be calculated using [13]:

$$HCT = \frac{mt^2 \times \rho \times C_P}{\pi^2 \times \alpha_T} \ln\left(\frac{8(T_M - T_{MD})}{\pi^2 (T_E - T_{MD})}\right) \tag{D.24}$$

where mt is the mold wall thickness (m), ρ is the density, α_T is the thermal conductivity(W/m·K), and T_M is the melting temperature of the material being molded (°C), and T_{MD} is the temperature of the mold (°C).

The total cycle time, *TCT* (sec/part), is then calculated using a correlation that factors in mold opening and closing times, mold cleaning, and a mold complexity factor [13]:

$$TCT = MCF \times [CT + 1.35 \times \text{HCT} + 0.0151 \times PW \times N_C + 8.87] \quad \text{(D.25)}$$

where *CT* is the compression time (sec/part) calculated using Eqn A.32, and *MCF* is the mold complexity factor.

The number of cycles per minutes, *CPM*, can be calculated as:

$$CPM = \frac{60}{TCT} \quad \text{(D.26)}$$

Table D.7 shows a breakdown of the variable costs and fixed costs associated with the process and their sum, the total fabrication cost.

Table D.7 Summary of breakdown of costs for baroplastic materials

VARIABLE COSTS	**per piece**	**per year**	**percent**
Material Cost	$0.017	$17,340.01	9.67%
Energy Cost	$0.013	$12,631.12	7.05%
Labor Cost	$0.098	$98,453.76	54.92%
Total Variable Cost	**$0.13**	**$128,424.90**	**71.64%**

FIXED COSTS	**per piece**	**per year**	**percent**	**investment**
Main Machine Cost	$0.011	$10,710.93	5.97%	$81,468.19
Auxiliary Equipment Cost	$0.002	$1,785.16	1.00%	$13,578.03
Tooling Cost	$0.020	$20,326.04	11.34%	$77,051.69
Fixed Overhead Cost	$0.012	$11,646.63	6.50%	
Building Cost	$0.005	$4,506.82	2.51%	
Maintenance Cost	$0.002	$1,866.45	1.04%	
Total Fixed Cost	**$0.05**	**$50,842.03**	**28.36%**	**$158,519.88**

Total Fabrication Cost	$0.18	$179,266.93	100.00%

Profit Markup	50%
Total cost of Part	$0.27 /part

The annual variable costs associated with the processing are determined from the equations below. The costs per piece are simply the costs per year divided by the annual production volume. The annual material cost, AC_{MA} ($/yr), is:

$$AC_{MA} = AMI \times P_{MA} \quad \text{(D.27)}$$

where P_{MA} is the raw material price ($/kg).

The annual energy cost, AC_{EN} ($/yr), is:

$$AC_{EN} = AE \times P_E \tag{D.28}$$

where P_E is the price of electricity ($/kwh).

The annual cost of labor, AC_L ($/yr), is:

$$AC_L = DW \times (APOT + 8 \times N_{IW} \times D) \tag{D.29}$$

where DW is the direct wage ($/hr).

The total equipment costs associated with the processing are calculated as described below. The total main machine cost investment, MMC_I ($), is:

$$MMC_I = C_{MC} \times N_{PM} (1 + C_{MI}) \tag{D.30}$$

where C_{MI} is the machine installation cost (%/machine).

The total auxiliary equipment cost investment, AEC_I ($), is:

$$AEC_I = C_{MC} \times N_{PM} (1 + C_{AEI}) \tag{D.31}$$

where C_{AEI} is the auxiliary equipment installation cost (%/machine).

The total tooling quipment cost investment, TEC_I ($), is:

$$TEC_I = C_{MD} \times N_T \tag{D.32}$$

The cost per year of the equipment (*MMC*, *AEC*, and *TEC*) was calculated by amortizing the total payment over the lifetime of the machine (15 years) for a given capital recovery rate (10%).

The annual building cost, *BC* ($/yr), can be calculated using as:

$$BC = C_{BS} \times (S_{MC} \times N_{PM} + S_{IW} \times N_{IW}) \tag{D.33}$$

where C_{BS} is the cost of renting building space.

The annual fixed overhead cost, *FOC* ($/yr), can be calculated using as:

$$FOC = (MMC + AEC + TEC + BC) \times OB \tag{D.34}$$

where OB is the overhead burden (% of fixed costs).

The annual maintenance cost, MC ($/yr), can be calculated using as:

$$MC = (MMC + AEC + TEC + BC) \times MIC \tag{D.35}$$

where MIC is the maintenance percent of the investment.

Finally, the total cost of the part is calculated as:

$$C_{PT} = FC \times (1 + PM) \tag{D.36}$$

where FC is the total fabrication cost ($/part) and PM is the profit markup (%/part).